AWSM 105-50/1

AIR WEATHER SERVICE MANUAL

FORECASTING UPPER-LEVEL WINDS

Part One

Forecasting By Vorticity Techniques

JUNE 1954

DEPARTMENT OF THE AIR FORCE

AIR WEATHER SERVICE
MANUAL No. 105-50/1

AIR WEATHER SERVICE
MILITARY AIR TRANSPORT SERVICE
UNITED STATES AIR FORCE
WASHINGTON 25, D. C. *June 1954*

Foreword

1. *General.* Air Weather Service Manual No. 105-50/1, "Forecasting Upper-Level Winds, Part One—Forecasting by Vorticity Techniques," is published for the information and guidance of all concerned.

2. *Scope.* This manual is the first part of a series to be published under the general heading of "Forecasting Upper-Level Winds." Several parts are in different stages of development. They include differential analysis in the troposphere, forecasting by kinematic techniques, and use of facsimile charts. To expedite their distribution they will be published as they are completed, without regard to sequence of subject material. Because of the gaps in basic knowledge of analysis and forecasting of winds above 300 mb, a series of technical reports is being prepared before any part of the manual dealing with the lower stratosphere is published. This technical report series has already begun with the appearance of AWS Technical Reports 105-86, 105-96, 105-107, and 105-108.

This manual (part one) discusses the use of the principles of absolute and relative vorticity in forecasting mid-tropospheric flow patterns for periods up to 72 hours. The early chapters deal with the so-called Rossby waves, or long waves in the westerlies, and supersede AWS Technical Report 105-80, which is now rescinded.

3. *Additional Copies.* Additional copies of this Manual may be requested from Headquarters, Air Weather Service, ATTENTION: AWSAD.

BY ORDER OF THE COMMANDER:

NICHOLAS H. CHAVASSE
Colonel, USAF
Chief of Staff

OFFICIAL:

LOUIS W. BERGER
Lt. Col., USAF
Adjutant

DISTRIBUTION:
"A" plus "E"

Contents

List of Figures

Section 1

THE VORTICITY CONCEPT AND THE LONG-WAVES IN THE WESTERLIES

1.0. Introduction. Many of those presently engaged in forecasting started their careers years ago when the main concern was with small areas and short-time intervals. These forecasters are likely to find it difficult to integrate into their daily routine an adequate consideration of the newer knowledge of the role of the broadscale features of the upper-flow patterns. Starr [31]* points out that this difficulty is a concomitant of the accidental way in which synoptic weather reporting networks developed. Not too long ago it was quite an achievement for a meteorologist to have at his command at forecast time a network of reports covering sufficient area to depict an entire cyclone. As a result the forecaster came to know the cyclone and associated upper-level troughs and ridges largely as phenomena that appeared to exist independently of developments in other sections of the hemisphere. The geographical extension of observations, especially upper-air observations, and the study of these observations by dynamic meteorologists has proved (what some had long suspected) that the cyclone (or anticyclone) is not independent of developments in other parts of the hemisphere; rather it constitutes a cogwheel in a larger mechanism. The relationship of the cyclone to the larger-scale-flow patterns must therefore be a part of the daily forecast routine if progress is to be made in forecasting the motions of cyclones and associated upper-air wind fields.

Upper-air flow patterns may be regarded physically as consisting of three fields: translation, rotation (vorticity) and deformation. Equations describing these motions are derived from the primitive hydrodynamical equations of motion. The practices of synoptic meteorology for many years have taken into account, at least empirically and qualitatively, the major effects of the fields of translation and deformation. But until about 1939 the effects of the vorticity field had not been considered in any effective way, either implicitly or explicitly. The study of hemispheric synoptic charts first led to a recognition of the similarity of the observed large-scale pressure patterns and the patterns obtained by integrating a simplified form of the vorticity equation [26], [27], [28]. In the last decade great strides have been made in the application of the vorticity equation to forecasting the motion of the large-scale-flow or "long-wave patterns." In addition, the vorticity approach is proving valuable in forecasting the shorter-waves. The results have been usefully applied to forecasts from 12 to 72 hours.

1.1. Organization of Manual. For the purposes of this manual, the discussion of the use of the vorticity equation will be divided into two parts:

a. The Large-Scale or Long-Wave Patterns, and

b. The Small-Scale Systems.

1.2. Vorticity.

1.2.0. Vorticity is the term used in fluid mechanics to describe the rotational motion of infinitesimal fluid elements. The synoptic meteorologist, however, is concerned with flow patterns of a scale found on a weather map, rather than the motion of individual fluid elements. Therefore we will be dealing here with mean vorticity averaged over an area whose linear dimensions are some hundreds of miles.

* Numbers enclosed in brackets are citations to references listed at the end of the Manual.

1.2.1. Relative Vorticity. The vorticity in a horizontal current can be broken down into two components, one due to the curvature of the streamlines, and the other due to the shear in the current. An example will illustrate this. Consider a flowing river. Place on the water two sticks, one perpendicular to the current (A) and one parallel to the streamlines of the flow (B) (see figure 1a).

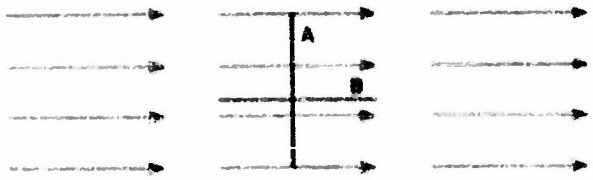

a.

Figure 1a. Schematic diagram illustrating zero relative vorticity.

1.2.1.1. If there is neither curvature nor shear in the current, neither of the sticks will alter its orientation relative to a fixed coordinate system as they are translated (transported) downstream. Such a current can be said to have no vorticity relative to the coordinate system. Now let us assume a horizontal shear exists in the current; as illustrated in figure 1b the shear results in stick (A) being rotated.

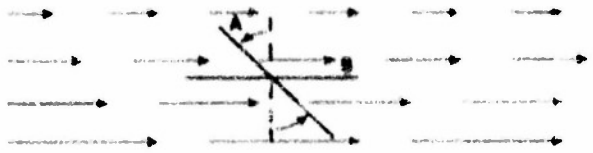

b.

Figure 1b. Schematic diagram illustrating positive (cyclonic) vorticity due to shear.

1.2.1.2. The vorticity in general is the sum of the rotations of the two sticks in relation to a fixed coordinate system. The vorticity is then said to be relative to this coordinate system. (Rotation is the change in angle per time unit.) In the case above only the stick normal to the streamlines will rotate and it is seen that the vorticity is equal to the shear of the current. Next assume that there is no shear but that the streamlines of the flow are curved. This results in a rotation of stick (B) as illustrated in figure 1c. Note that stick (A) does not rotate, since the shear is zero.

1.2.1.3. For daily operational use in weather analysis and forecasting, the relative vorticity field

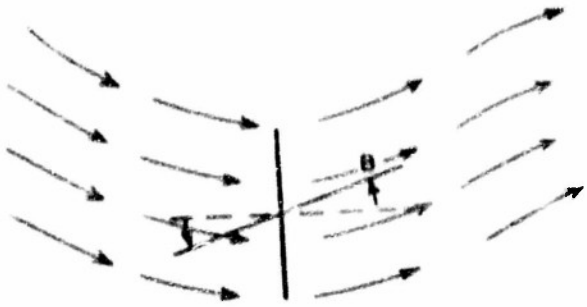

c.

Figure 1c. Schematic diagram illustrating positive (cyclonic) vorticity due to curvature.

of atmospheric flow patterns (i. e. relative to the earth's surface) may be evaluated from the curvature and spacing of contours on constant-pressure surfaces.

1.2.2. Absolute Vorticity. However, the quantity which appears in the vorticity equation is the absolute vorticity. The vorticity equation, being derived from Newton's Second Law, of motion, must contain terms describing motion with reference to celestial coordinates, i. e., with respect to the earth's orientation in space rather than with respect to the earth's surface. Since the earth is a rotating spheroid, all points on its surface except those on the equator, have a component of rotation around the local vertical. The magnitude of this component of rotation is a function of latitude and is equal to the Coriolis parameter ($2\,\Omega \sin \phi$). The *absolute vorticity* is thus defined as the sum of the Coriolis parameter and the relative vorticity.

1.3. Larger-Scale Patterns. Rossby investigated means of obtaining an equation which would give the speed of movement of large-scale waves in the atmosphere. By "large scale" he had in mind those waves which were of 40 to 120 longitude degrees in length. To obtain the wave speed, he used the vorticity equation with several simplifying assumptions some of which are severe [26]. It is important to know what most of these assumptions are. The ones discussed below are those with which we are directly concerned when applying the long-wave or Rossby equation to forecasting. Rossby considered that the wave motion was taking place in an atmosphere with no horizontal temperature gradient (winds constant in direction and velocity with height from surface to top of atmosphere). This is called a *single-layer barotropic atmosphere*. For the practical implication of this assumption

see paragraph 2.0. Rossby also assumed that the flow patterns in this barotropic atmosphere contained no lateral shear. This means the relative vorticity is given only by the curvature of the streamlines. Another assumption was that the flow pattern is sinusoidal and of small amplitude (see par. 2.16.2.). Further, he assumed that the absolute vorticity remained constant with time which means that changes of relative vorticity (i. e., of curvature of the streamlines) occur only when the Coriolis parameter changes.

The equation for the wave speed that Rossby derived is

(1) $c = U - \beta L^2/4\pi^2$, where

c = wave speed,
U = zonal wind speed (west-wind speed),
L = actual observed wave length, and
β = rate of change northward of the Coriolis parameter = $\frac{2\omega(\cos\phi)}{R}$, in which
ω = angular speed of the earth,
ϕ = latitude, and
R = radius of the earth.

It can be seen from equation (1) that the wave speed is a function of the speed of the west wind, the wave length and latitude. Determination of these quantities is discussed in section II.

For stationary waves ($c=0$), equation (1) may be written in the form

(2) $U = \beta L_s^2/4\pi^2$,

where L_s (the stationary wave length) is a function of the strength and position of the zonal wind stream, and may be used conveniently to represent the wave length of a hypothetical stationary wave. Eliminating U between equations (1) and (2), c becomes

(3) $c = \frac{\beta}{4\pi^2}(L_s^2 - L^2)$.

In equation (3) the wave speed is given as a function of the difference of the squares of the hypothetical-stationary (L_s) and observed (L) wave lengths, and of the latitude. Further, comparison of these two wave lengths will indicate whether the wave is

stationary,	($L_s = L$, $c = 0$),
progressive,	($L_s > L$, $c > 0$),
or retrograde,	($L_s < L$, $c < 0$).

In applying the Rossby equation for the motion of atmospheric wave patterns, it is necessary to keep in mind the fact that the motion described is that of large-scale systems, i. e., of waves whose wave length and amplitude are large enough that the variation of the Coriolis parameter with latitude is of importance in determining the wave dynamics. These are called the *long waves* (or *major waves*) and may be defined as those atmospheric waves of relatively large amplitude which exist in depth through the troposphere and lower stratosphere (see Rossby [27], Namias [18], Fultz [12], and Crossman [7]). They are associated with warm tropospheric ridges and cold tropospheric troughs found in the mid-latitude westerlies. Their horizontal amplitude increases with height in the troposphere, reaching a maximum at the tropopause, and decreases with height in the stratosphere. Their motion is slow, seldom exceeding 13 long. deg. per day. They often remain quasi-stationary for periods up to a week or more. Due to this slow motion they often appear as waves of large amplitude on 5-day mean upper-level charts.

The identification of the long waves at low levels, particularly at 700 mb and below, is made difficult by the presence of the rapidly moving, smaller-scale, warm troughs and cold ridges (*minor waves*). Since, the minor waves decrease in amplitude with height the best level for the identification of the long waves is near the tropopause (300 mb or 200 mb) where their amplitude is greatest. Owing to the lack of high-level data over much of the hemisphere, the 500-mb chart is currently used as the basic chart for the study and analysis of the long-wave patterns.

In order to use the equation (3) as a tool for forecasting the long-wave motion it is necessary to have some idea of the future variations of L_s and of L. The problem of forecasting L_s is a very difficult one, and has not been solved satisfactorily. However, it has been shown by Crossman [7] that variations of L_s are gradual, having little effect on a forecast for 1 or 2 days. Although persistent trends in the values of L_s can occasionally be detected and extrapolated, most of the short term (12 hr or 24-hr) variations in L_s shown by the computations are due to irregularities in the analysis, caused mainly by lack of data, and are not significant. In fact, one can often obtain the most representative value of L_s by averaging the values computed from three or four successive 12-hr maps. In the regular forecast routine then, L_s may be considered as nearly constant.

The variation of actual wave-length can be forecast to a certain extent by a treatment in which L is assumed to have a continuous variation along the x (west-east) axis (Crossman [8]). The practical application of variations to actual wave-length are discussed in section II.

1.4. Smaller-Scale Patterns. The use of advection of relative vorticity (in which both shear and curvature are considered) is helpful in forecasting the smaller-scale wave patterns. The principle involved is that the motions of the smaller-scale troughs and ridges in the mid-troposphere are closely associated with the advection of the 500-mb relative-vorticity field. This will be discussed in section III.

Section II

APPLICATION OF THE EQUATIONS FOR WAVE MOTION TO THE SYNOPTIC CHARTS

A. GENERAL PRINCIPLES

3.0. Equivalent Barotropic Level. The principal difficulty encountered in the application of equation (3) to the synoptic charts is caused by the increase of wind with height in the actual baroclinic atmosphere, since equation (3) was derived for a single-layer barotropic atmosphere. This difficulty is surmounted by the application of the computations to the equivalent barotropic level. A discussion of this question has been given by Charney [3] and by Charney and Eliassen [5]. They have shown that "an equivalent-barotropic atmosphere can be defined, whose motion corresponds to the motion of the baroclinic atmosphere at a certain level." A considerable number of investigations by Charney [3], Charney and Eliassen [5], Charney [4], Cressman [7], and Palmén and Newton [22] has shown that the level in question is very near 600 mb. In forecasting practice then, the stationary wave length is evaluated from the winds at 600 mb. This is done by working down from the 500-mb surface, as described in the Appendix (par. A1.9).

3.1. Criteria for L_s. In determining values of L_s from the upper-air charts, the following criteria should be used:

a. The area on the chart, over which L_s is computed and to be applied, should contain a well-defined and continuous belt of westerlies, in which the long-wave pattern in question is located.

b. The area over which L_s is computed should include about 120 long. deg. Computations on a small scale, e. g., for sectors of about 50 long. deg., will include less than one wave length and will be unrepresentative of large-scale conditions. They will unduly emphasize relatively local conditions in a major trough, or in a major ridge. On the other hand, computations that are made around the hemisphere, such as for the zonal wind speed (U in eq. 2) which is averaged for fixed latitude and longitude sectors (see Appendix), will not be very useful in view of the polar eccentricity and wave form of the westerlies. For example, it is observed that the westerlies over the USSR are usually much farther north than those over the Pacific. Under those conditions the computation of the zonal wind speed averaging around the hemisphere at one latitude would not reflect the full strength of the westerlies. Therefore, a 120-degree sector has been found the best choice in practice. If computations of U and L_s on a hemispheric scale are desired, they can be made separately for three 120 long.-deg. sectors.

c. L_s should be computed for a series of 5°-latitude belts covering a range sufficient to include the belt of westerlies (usually 25° 60° N). Next one must choose the particular L_s which best represents the maximum core of the westerlies. However, when the waves of the current have unusually large amplitude, none of the 5°-latitude belts for the 120° sector may be sufficiently representative to be useful. A judicious selection of the 120 long.-deg. sector is needed to fulfill this requirement satisfactorily.

d. It is sometimes observed that two currents of westerlies, both having considerable strength at 500 mb will be present at different average latitudes. When this occurs, the computation of the stationary wave length for this sector may be unrepresentative of either current. In any case it is advisable to inspect the upper-air charts closely

to see that the latitude at which the stationary wave length is computed corresponds to a well defined current of westerlies.

2.2.6. Verifications. Several verifications have been made of equation (3) for periods of from 24 to 72 hours. It has been shown by Crossman [7], and also by some unpublished verifications that when equation (3) is used on the major waves, with L_s computed from the winds at 600 mb, the average absolute error (i. e., without regard to sign) in the verification of a 24-hour forecast of trough displacement is between two and three longitude degrees. For periods in excess of 24 hours, the change of wave length with time must be taken into account. This can be done by computing the total displacement in 24-hour steps. For such a computation it is necessary that at least several of the long waves show on the chart.

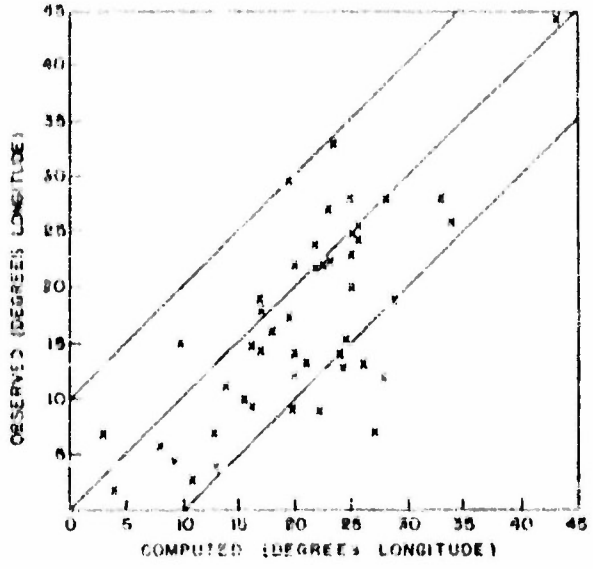

The computed versus observed 3-day displacement is shown for each test. The outer two slanting lines encloses all the points having an error of less than 10 long. deg.

Figure 2a. Results of 50 tests of trough motion, computed from equation (3), taking into account the three change wave lengths for 72-hour periods.

2.2.7. A verification of the Rossby equation taking into account the change of wave length with time for 72-hour periods, as described by Crossman [8], gave the results shown in figure 2a. Fifty computations of 3-day trough displacements were made, but with several restrictions. The first restriction was that the situations were selected so as to include only cases where the long wave pattern was conserved through the period. A change in the general structure of the pattern or a change of the wave number (total number of major waves around the hemisphere) during the period was considered sufficient to preclude a test. Also excluded from the testing were situations where the measurement of wave lengths or of displacement was difficult due to the obscuring of major troughs by minor troughs of unusually large amplitude. This eliminated those patterns where the eastern trough retrograded during the test period, since the large amplitude of the minor troughs present during the retrogression of a major trough usually made the measurement of trough speed impossible.

2.2.8. The average absolute value of the errors represented in figure 2a is six long. deg. Another test was made on the same data by tripling the trough displacement observed in the 24-hour period preceding the forecast period and using the resulting value as a forecast. This method could be evaluated on only 42 of the patterns. The previous 24-hour trough displacement could not be evaluated for eight patterns due to various reasons. This method of forecasting gave an average absolute error of 13 long. deg. for the 3-day displacement.

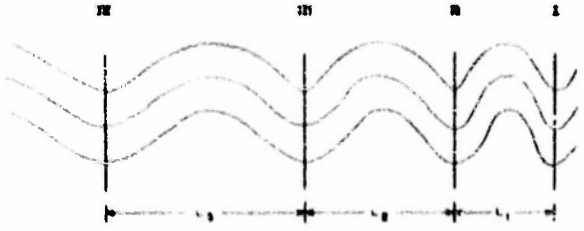

Figure 2b. Hypothetical long-wave pattern as seen on the 500-mb chart with wave length increasing upstream.

2.3. Effect of Variation in Wave Length. The method of taking into account the variation of wave length when computing displacement of troughs beyond 24 hours follows.

a. Increasing wave length upstream tends to decelerate trough movement. In figure 2b, the fact that L_3 is greater than L_1 will decelerate the movement of trough I. Considering a constant zonal wind (i. e. constant stationary wave length) in equation (3), it can be seen that trough I will move farther in a 24 hour period than trough II. This is because $(L_s^2 - L_1^2)$ is greater than $(L_s^2 - L_2^2)$. This differential motion of troughs I and II will result in L_1 increasing with time and a corresponding decrease in $(L_s^2 - L_1^2)$. Since the speed of trough I is determined from equation (3) by $(L_s^2 - L_1^2)$, a de-

crease of this quantity will result in trough I slowing down. Similarly, trough II will decelerate since L_2 is less than L_3.

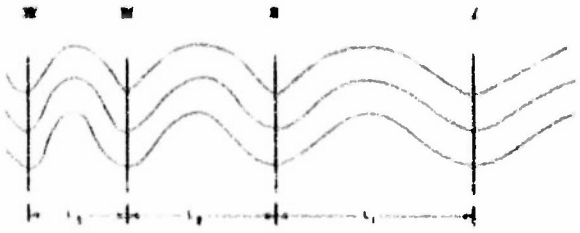

Figure 2c. Hypothetical long-wave patterns as seen on the 500-mb chart with wave length decreasing upstream.

b. *Decreasing wave length upstream tends to accelerate trough movement.* Following the same general reasoning as in (a) above, it can be seen in Fig. 2c that $(L_3^2 - L_1^2)$ is less than $(L_3^1 - L_2^1)$ which results in L_1 decreasing and $(L_3^2 - L_1^2)$ increasing with time. This, of course, accelerates the movement of trough I. Similarly, trough II will accelerate when $(L_2^2 - L_3^2)$ is less than $(L_2^1 - L_3^1)$.

The effect of increasing or decreasing wave lengths upstream can be obtained by computing trough displacement in 24-hour steps. This can be done by using L_1 (in figure 2b or 2c) for computing the displacement of trough I for the first 24 hours, and by using L_2 for trough II and L_3 for trough III. The resulting new trough positions will then be associated with new values of wave length at the end of 24 hours. However, in order to obtain the wave length between troughs III and IV after 24 hours, some assumption about the motion of trough IV is necessary. If none is made, the displacement of trough III for the second 24 hours can not be computed. The displacements of troughs I and II for the second 24 hours can be computed by use of the new values of L_1 and L_2. If a new position for trough IV after 24 hours is assumed by some means (not discussed here), a new value for L_3 is available, and a position for trough III can also be computed at the end of the second 24-hour period. The same process can be repeated giving the trough positions at the end of the third 24-hour period. For example, the distance between troughs I and II at the end of 48 hours would give the new wave length to be used in obtaining the displacement of trough I for the third 24-hour period. If some motion is assumed for trough IV for the first 48 hours, computations for the entire three periods can be made for troughs I, II, and III.

If no assumption is made about the motion of trough IV, 48-hour displacements can be obtained only for troughs I and II, and a 72-hour displacement only for trough I. However, if the regular wave-pattern extends completely around the hemisphere, no assumption about the motion of any trough need be made.

B. IDENTIFICATION OF THE LONG WAVES

2.4.0. Space-Mean Charts. As pointed out in section I, par. 1.3, identification of the long waves is made difficult by the presence of the rapidly moving minor waves. The space-mean chart, developed by Fjörtoft [11], has proved very useful in identification of the long waves. This chart is obtained* by averaging a given 500-mb chart displaced a certain distance in four different directions, to the ends of the grid shown in figure 3. If four copies of the same 500-mb chart were placed at the ends of this grid, added together graphically, and the sum divided by four, the resulting chart would be the space average desired.

2.4.1. To interpret the resulting space-mean chart, one should visualize the grid ABCDE of figure 3 laid upon any point of the original chart. The 500-mb heights at the ends of the grid are Z_A,

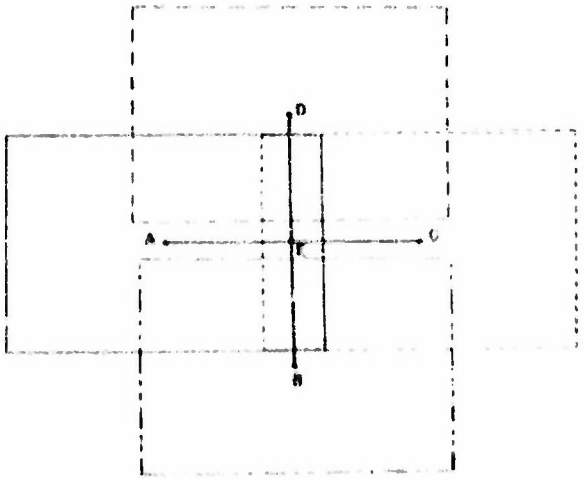

The five rectangles represent four different locations on the original 500-mb chart.

Figure 3. Space-mean grid (AE = BE = CE = DE = 360 nautical miles).

* For the details of constructing this chart, see the appendix.

Z_B, Z_C, and Z_D, with the height at E being Z_E. It can be seen that the height at the corresponding point E on the space-mean chart is $\frac{1}{4}$ (Z_A + Z_B + Z_C + Z_D), which is called Z_E. The space mean chart is often called the $\bar{Z}$ ("zee bar") chart. It has been determined from many considerations that a grid size (distance from E to any of the outside points) of 3001 nautical miles is the most useful. With a grid of this size one finds that the small-amplitude, rapidly moving disturbances are averaged out and do not appear on the space-mean chart, leaving the large-scale slowly moving systems, including the long waves. In the long-wave examples which follow, the $\bar{Z}$ charts will be shown as well as the original 500-mb charts.

2.5. Height Profiles. The construction of height profiles has also been found helpful in the identification of the long wave patterns. Height profiles can be drawn in the form of a graph of the latitude of a given 500-mb contour, such as 18,500 feet, against longitude, or in the form of a graph of 500-mb height at a given latitude circle against longitude, or the "trough-and-ridge-diagram" suggested by Hovmöller [14]. These profiles represent the large-scale patterns in easily visualized form, as will be seen from the examples.

C. EXAMPLES

2.6.0. Progression of the Long Waves. Progression (eastward movement) of the long waves is usually found in association with relatively short wave-lengths and well-defined major troughs and ridges in the middle and upper troposphere. At the surface, there are usually only one or two prominent cyclones associated with each major trough aloft. Under the forward part of each major ridge there is usually a well-developed surface anticyclone, moving toward the east or southeast. The 24-hour height changes at upper levels usually have a one-to-one association with major troughs and ridges (e. g., motion of maximum height fall and rise areas associated respectively with major trough and ridge motion). The tracks of the height-change centers depend on the movement and changes of intensity of the long waves, and often seem somewhat erratic.

2.6.1. The situation of 13–15 January 1951 (figs. 4a-j), is presented as AN EXAMPLE OF A PROGRESSIVE LONG-WAVE PATTERN. Although the analysis of the long waves is made on the 500 mb chart, the two surface charts, figures 4b and 4g, are shown as an indication of the relation of the surface patterns to those in the upper air. The computed values of the zonal wind speed and stationary wave length are shown in figure 4d. There is one predominant west-wind current in the Pacific, with maximum speeds at 40–45°N. At the west coast of North America, this current splits into two maxima. A narrow current flows across Canada, while a broader one is found over the southern United States and continuing across the Atlantic. The map will therefore be considered to contain a predominant current of westerlies with average latitudes of 40–45°N in the Pacific and 35–40° N over the United States and the Atlantic. The northern current across Canada will not be considered in this illustration. At the computation latitudes, mentioned above, the major troughs are found at 137°E, 161°W, 109°W, and 59°W. (See fig. 4a.)

2.6.2. In this example, there is little room for doubt as to the location of the major troughs. The space-mean chart, figure 4e, presented for comparison, clearly shows the long-wave pattern at middle latitudes. The values of the stationary wave length from figure 4d are 91 long. deg. for the Pacific and 71 long. deg. for the United States and the Atlantic. One of the long waves overlaps the two zones used for computation—from the Gulf of Alaska to the Rocky Mountain area. A value of L_s = 81 at 40°N, which is an average value for the two zones, is used for the first 24-hour period. For the second 24-hr period this wave is almost entirely within the eastern computation zone and the value of L_s = 71 degrees is used. The results of the computations are indicated in figure 4c. A constant value of L_s = 62 long. deg. was assumed for the Pacific (i.e., the 137° E trough progresses at the same rate as the 161° W trough) in order that a 48-hour position could be computed for the Gulf-of-Alaska trough. If the East-Asia trough had been assumed to remain stationary, a smaller eastward motion would have been indicated for the Gulf-of-Alaska trough for the second 24-hour period.

2.6.3. The maps for the end of the 48-hour period, on 15 January 1951, are shown in figures 4f, 4g, and 4h. It is evident that the long waves had a rapid eastward motion through the period. Although the orientation with respect to the meridians of some of the features (particularly the Gulf-

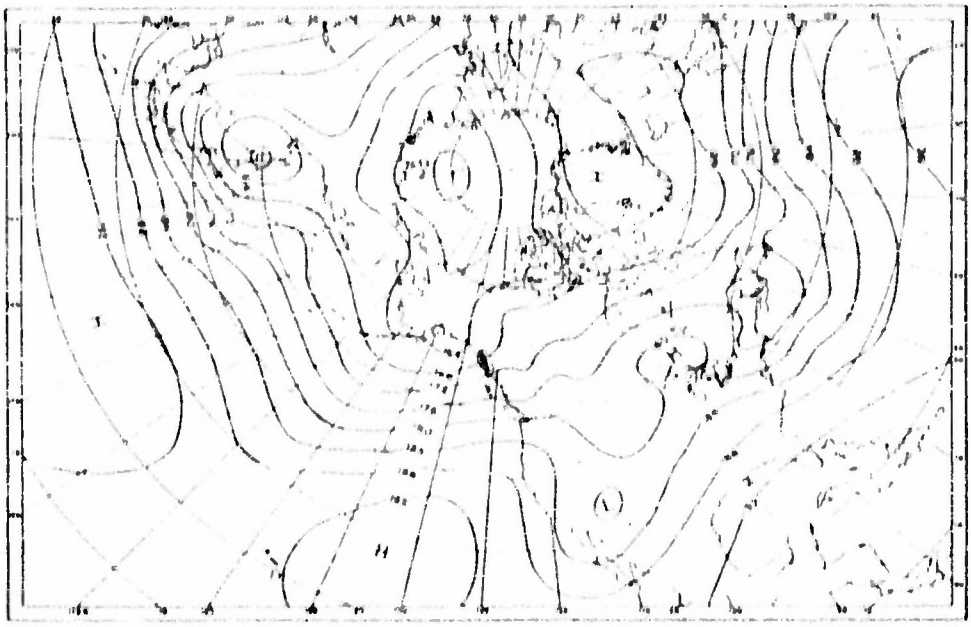

Figure 4a. 500-mb chart, 0300 GCT, 13 January 1951.

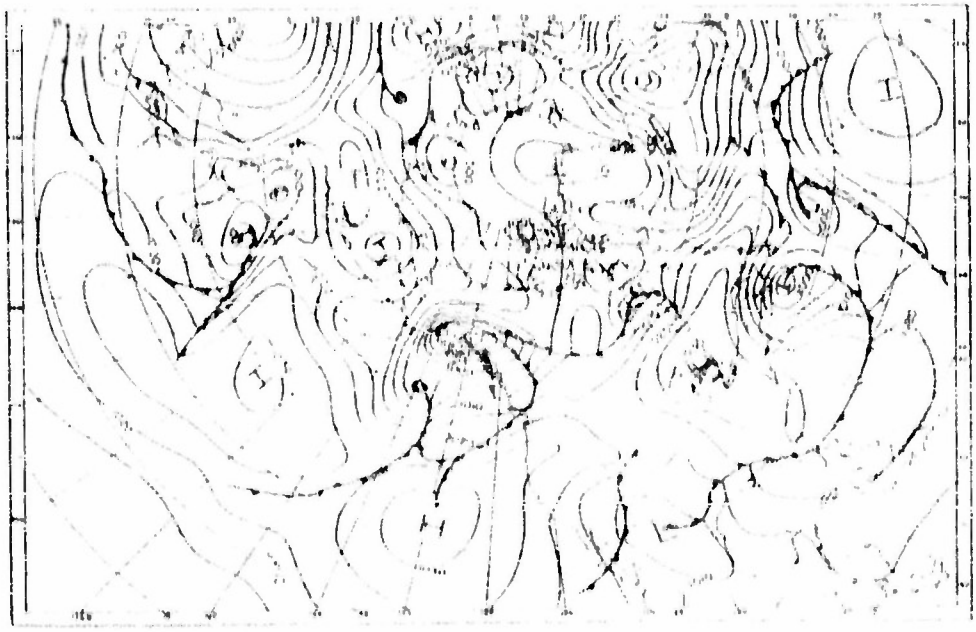

Figure 4b. Sea-level chart, 0030 GCT, 13 January 1951.

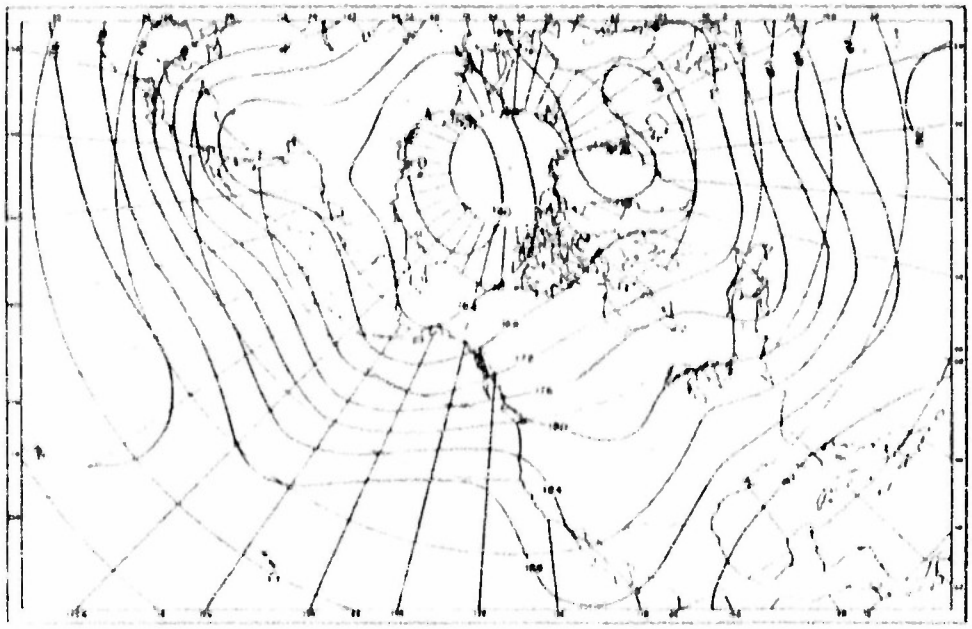

Figure 4c. Space-mean 500-mb chart, 0300 GCT, 13 January 1951.

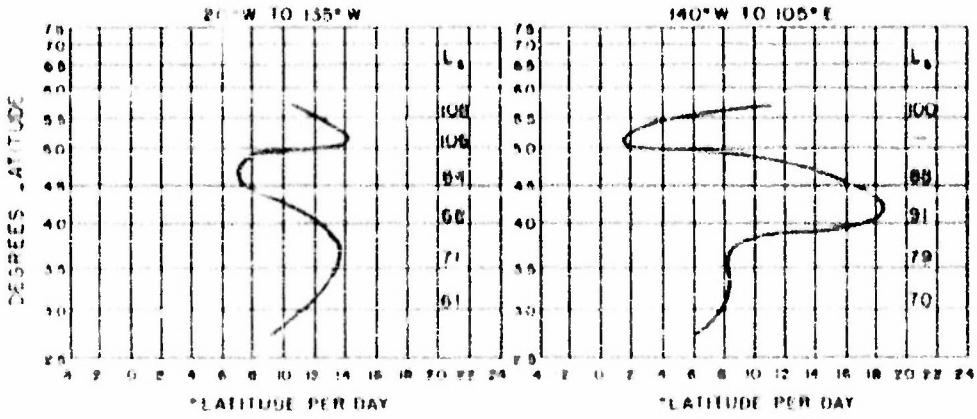

Values of stationary wave lengths computed for each 5° latitude band are listed at the appropriate latitudes on the graphs. The profiles and stationary wave lengths are for 500 mb, 0300 GCT, 13 January 1951.

Figure 4d. Zonal wind profiles giving west wind component at 6°N mb in units of latitude degrees per day (units of 60 nautical miles per 24 hours), as a function of latitude.

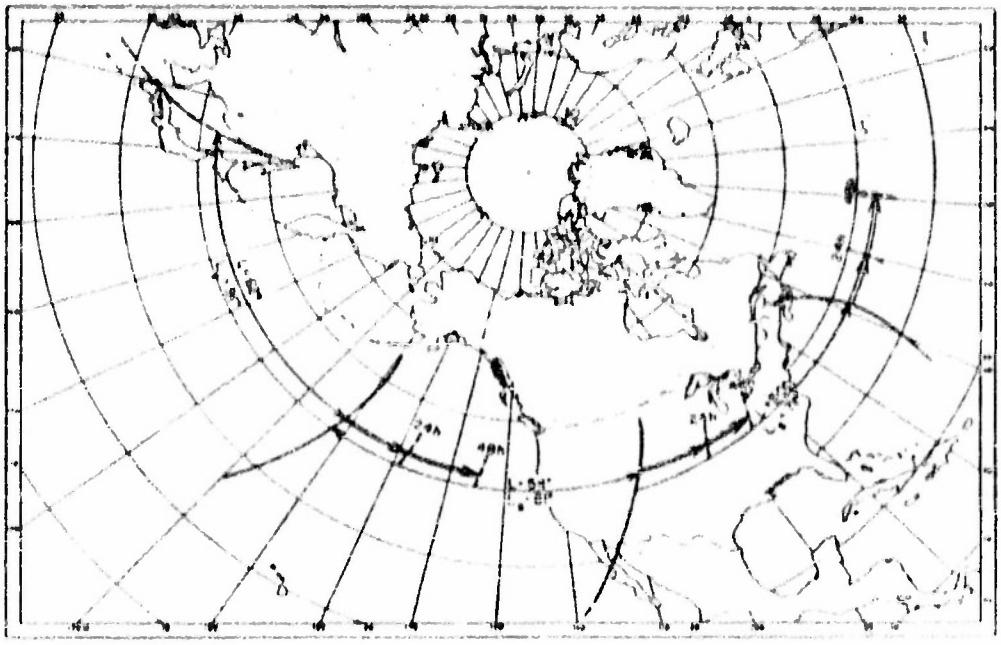

Double arrows show computed major trough positions after 24 hours and 48 hours.

Figure 4e. Schematic chart with positions of major troughs and values of actual and stationary wave lengths for 500 mb, 0300 GCT, 15 January 1951 (corresponding to fig. 4a).

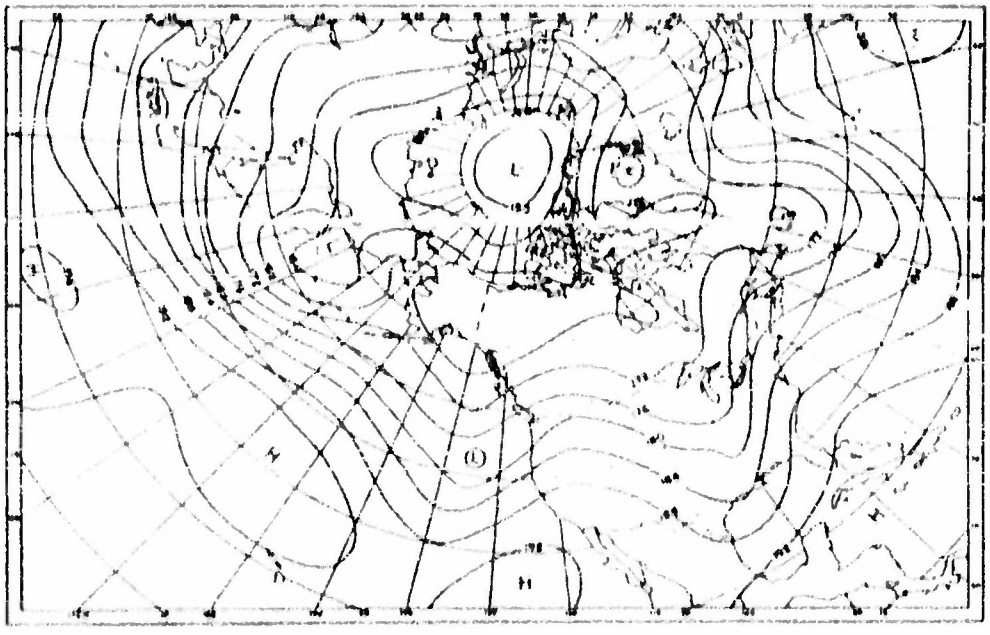

Figure 4f. 500-mb chart, 0300 GCT, 15 January 1951.

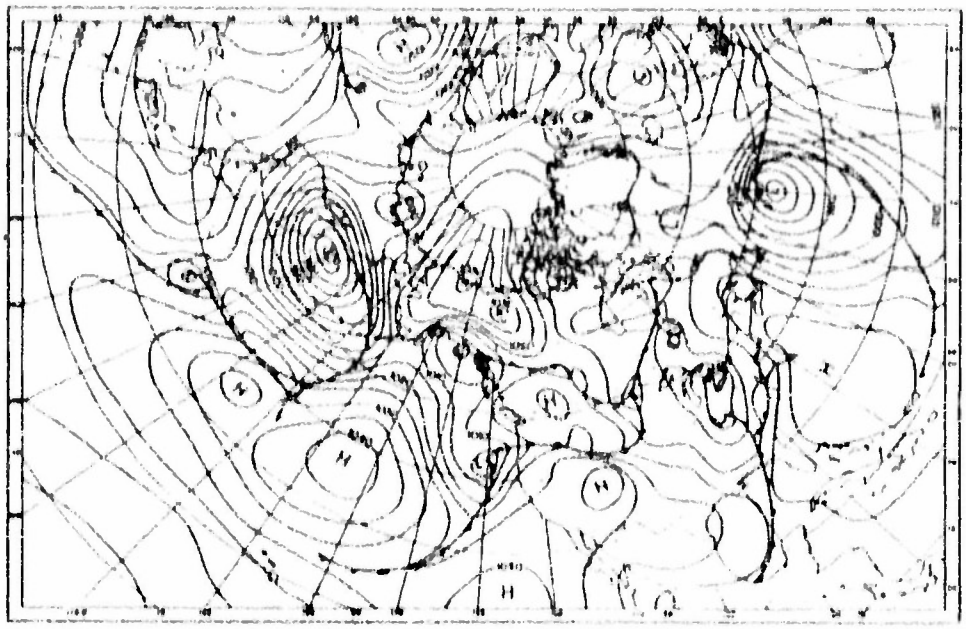

Figure 4g. Sea-level chart, 0300 GCT, 15 January 1951.

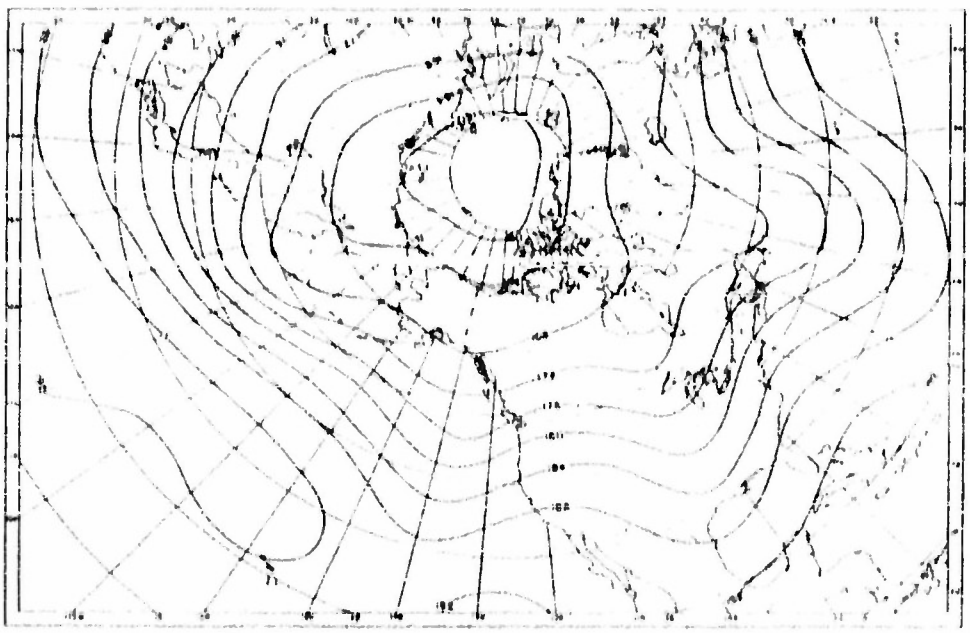

Figure 4h. Space-mean 500-mb chart, 0300 GCT, 15 January 1951.

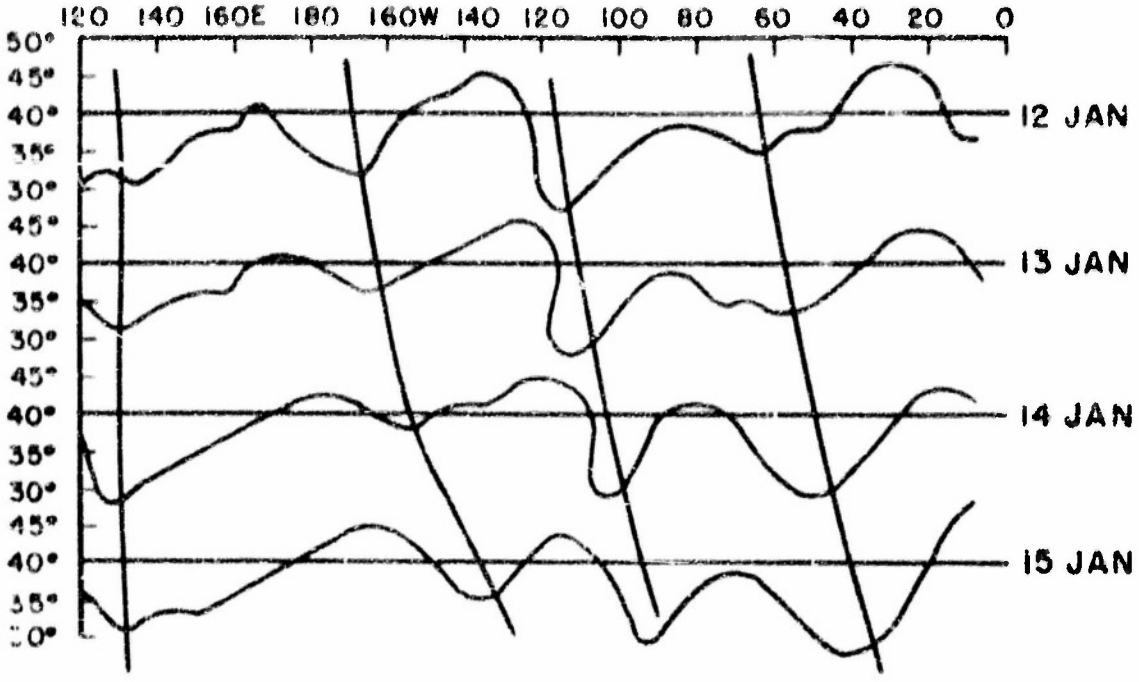

Figure 41. Profile of the 18,000-foot contour at 500 mb, 13-15 January 1951. Quasi-vertical lines represent major trough positions.

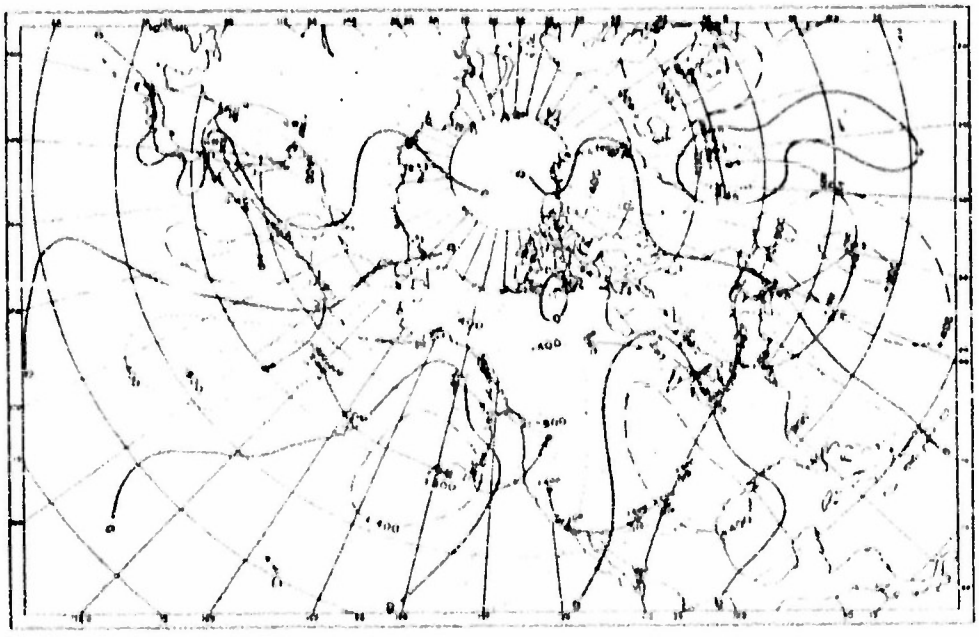

Rises are indicated by dashed lines and falls by dotted lines. Successive positions of the centers are indicated by the small circles. The number above each circle refers to the intensity of the change center. The number below each circle refers to the date, e. g., "15" means that the circle gives the position of the change center from 14 to 15 January 1951.

Figure 42. 24-hour 500-mb height changes, 0300 GCT, 15-16 January 1951, with trajectories of change centers.

of-Alaska trough) changed, the movements at the computation latitudes were reasonably close to the computed motions. The location and progressive motion of the long-wave pattern are also clearly shown by the profiles in figure 4i.

2.6.4. The sea-level maps show a significant eastward motion of the large anticyclones and of the major cyclonic regions as the upper long-wave pattern moved toward the east. One of the most interesting developments is the appearance of a series of pronounced anticyclones in a line from north to south over western North America which took place as the major ridge aloft moved in from the Gulf of Alaska over the cold air in the low levels over the continent. This situation is characteristic of the general type where the long waves are progressive, in that the surface anticyclones and cyclones are well developed, and the major troughs and ridges aloft are pronounced and easily recognizable.

2.6.5. It is of interest to compare the behavior of the 24-hour change patterns, which are often used in prognosis of the upper air, with the long-wave patterns. (See fig. 4.) The west-east component of the motion of these centers corresponds, to a certain extent, with the motion of the long waves; but the north-south component of their motion depends on the filling or deepening of the major troughs and ridges. As a result, the movement and intensity changes of the change patterns seem to be irregular.

2.7.0. Stationary Long-Wave Patterns, once established, usually persist for a number of days. The upper-air flow associated with the long-wave pattern constitutes a steering pattern for the smaller-scale disturbances. These small-scale troughs and ridges, with their associated height-change patterns and weak surface systems, move along in the flow of the large-scale, long-wave pattern. As shown by Namias [18], Pultz [12], and others, the minor troughs intensify as they move through the troughs of the long waves and weaken as they move through the ridges of the long waves. The same changes of intensity occur in those sea-level troughs or pressure centers which are associated with minor troughs. Partly as a result of the presence of these smaller-scale systems, the troughs and ridges of the stationary long waves are often spread out and hard to locate exactly.

2.7.1. THE SITUATION OF 15–17 DECEMBER 1950, is shown in figures 5a–i. In figure 5b the predominant current of westerlies is found at middle latitudes. A second, much weaker, current meanders across the map at much higher latitudes. The stationary wave length (figure 5a) for the North American and Atlantic zone is 76 long. deg. at 40–45°N in association with a maximum of the zonal wind. For the Pacific section of the map, the stationary wave length continues to increase for a considerable distance north of the maximum west wind. The increase is due to the presence of the second weaker wind current at a higher latitude across Sakhalin and the Bering Sea. As indicated by the criteria discussed in the APPENDIX, the value of 78 long. deg. which is found at the latitude of maximum west wind at 40–45°N, is the best value for the stationary wave length. This is confirmed by appearances of the map, since the belt 40°N to 45°N goes through the center of the west-wind current.

2.7.1.1. The identification and measurement of the actual long-wave pattern on 15 December is more difficult than in the previous example, due to the complex structure of the pattern in the east half of the map. However, the space-mean chart for 15 December, figure 5d, shows an easily identified long-wave pattern. At the latitudes discussed above, the actual wave lengths on 15 December are 74 long. deg. in the Pacific and approximately 70 long. deg. for the United States. Both of these values are just slightly less than the values of the stationary wave length. As indicated by the above data, little motion should be expected of the major troughs in the next 2 days.

2.7.1.2. The 500-mb chart for 17 December 1950 (fig. 5e) shows a notable similarity to the one for 15 December 1950 (fig. 5b). The major trough over eastern North America is still spread out, its location being difficult to specify except on the space-mean chart (fig. 5g). The major trough in the Gulf of Alaska has not moved, and the major trough over the sea of Japan has retrograded about 10 long. deg. The major ridge over North America is well defined on both maps. The minor trough seen superimposed on the Pacific major ridge on the 17th was different from the one in the same place on the 15th, both of which were moving rapidly eastward at map time. The stationary character of the long-wave pattern through this period is evident from a comparison of the two space-mean charts (figs. 5d and 5g) and from the profiles of the 18,400-foot contour at 500 mb, shown in figure 5h.

2.7.1.3. Although little change occurs on the upper-air charts for this period, pronounced changes

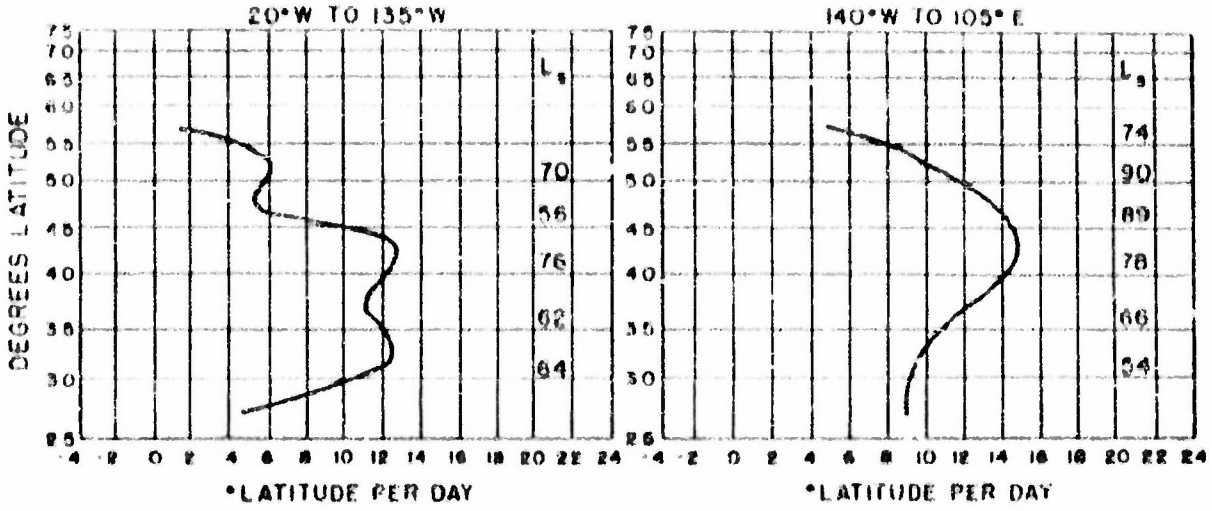

Figure 5a. Zonal wind profile and stationary wave lengths, 0600 GCT, 15 December 1950.

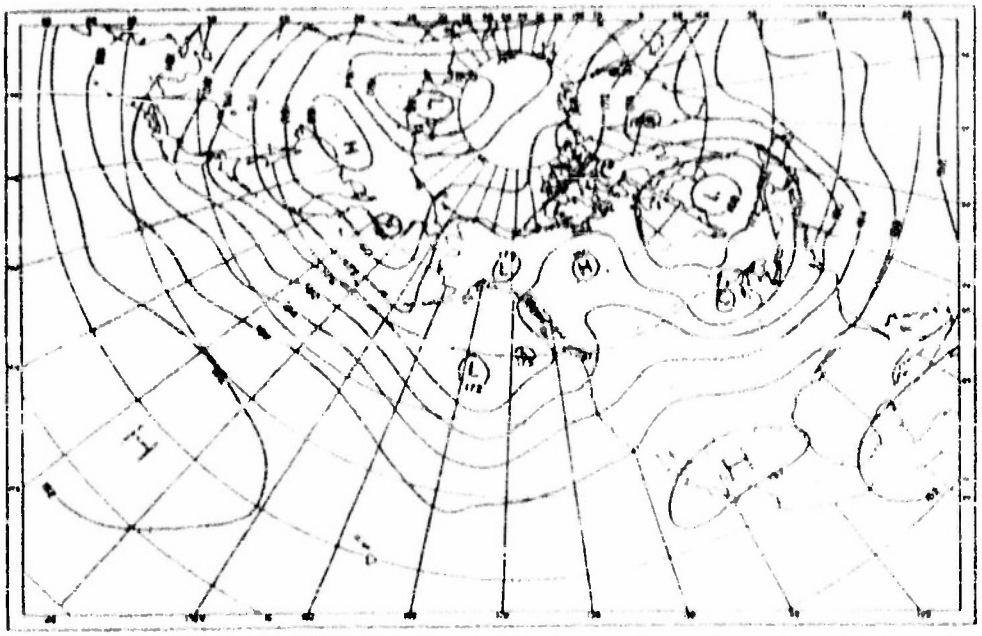

Figure 5b. 500-mb chart, 0600 GCT, 15 December 1950.

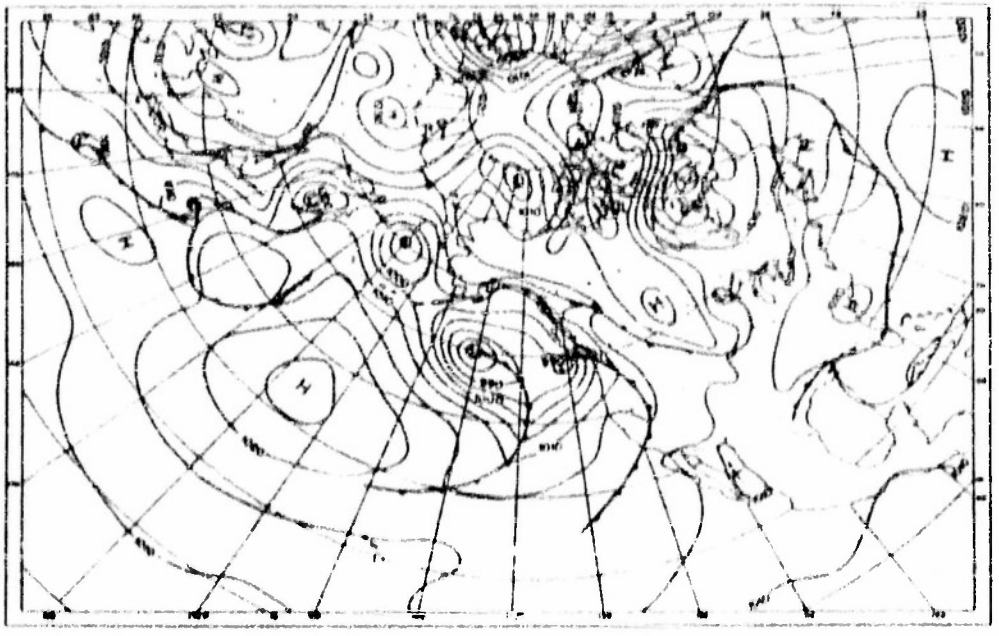

Figure 6c. Sea-level chart, 0030 GCT, 15 December 1960.

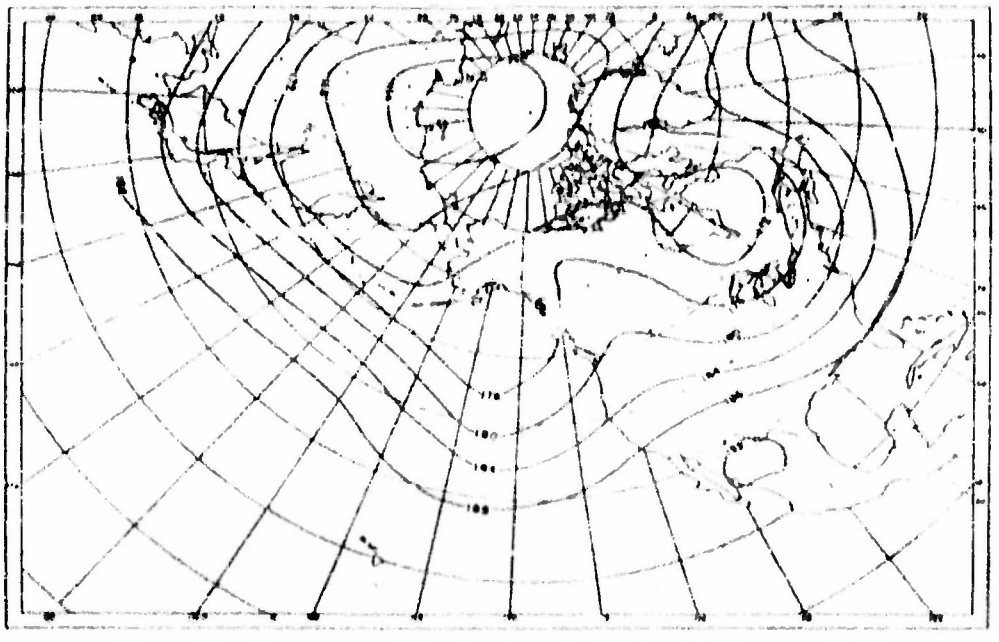

Figure 6d. Space-mean 500-mb chart, 0300 GCT, 15 December 1960.

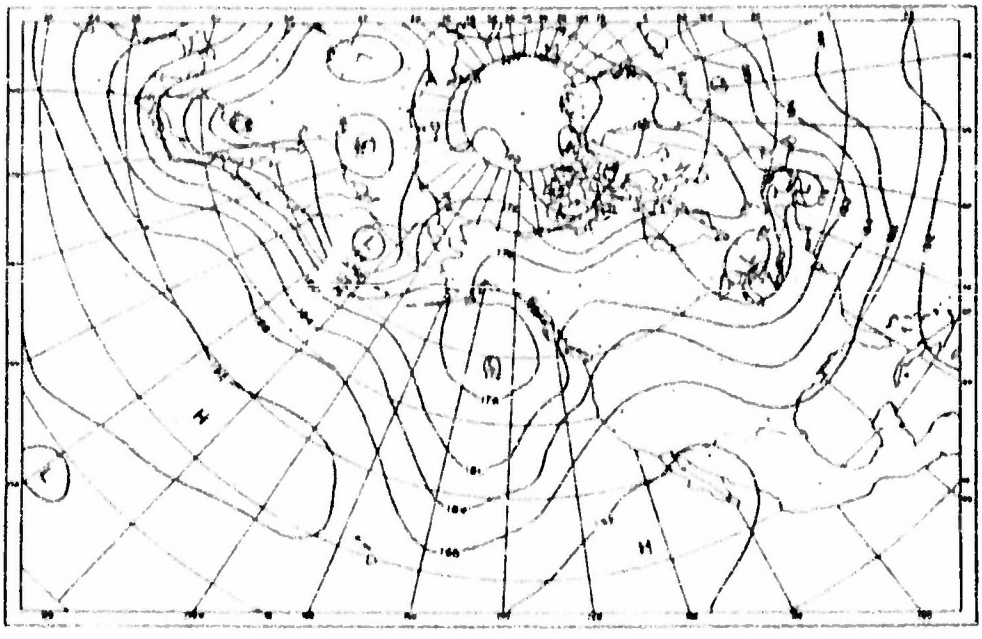

Figure 5e. 500-mb chart, 0400 GCT, 17 December 1950.

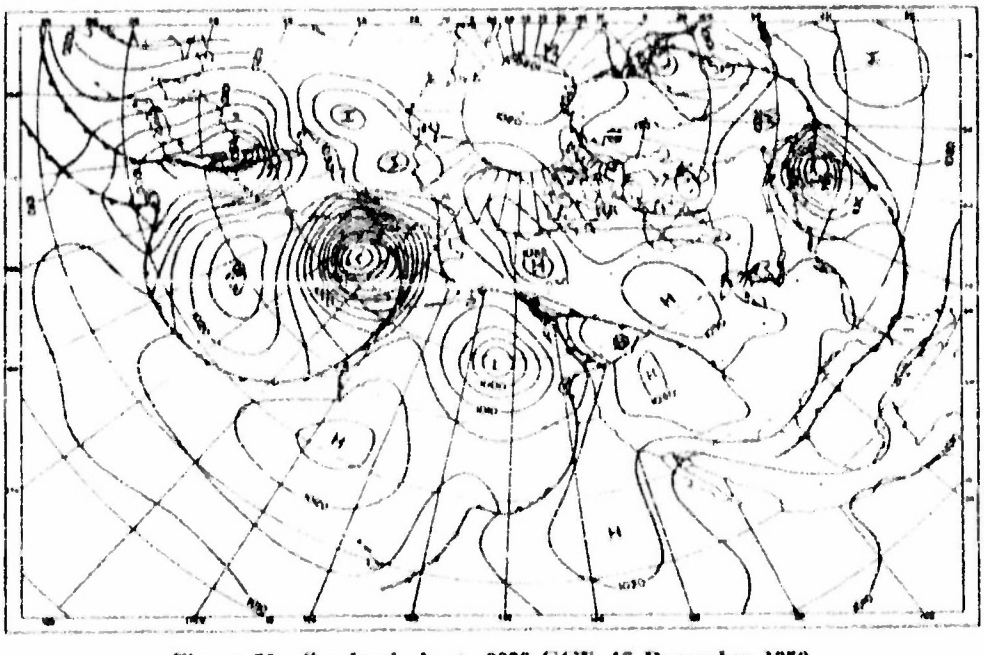

Figure 5f. Sea-level chart, 0030 GCT, 17 December 1950.

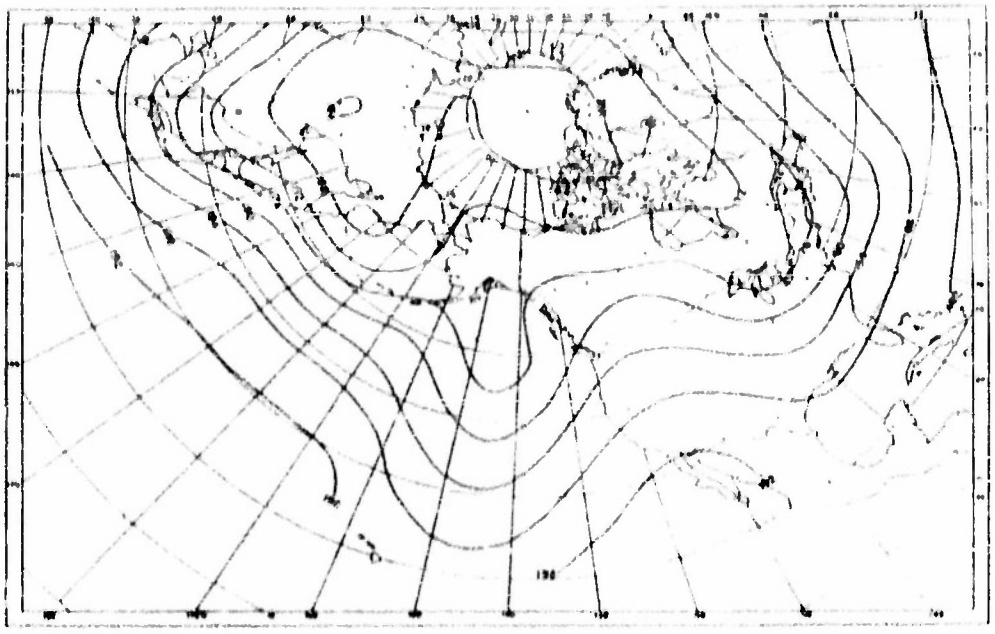

Figure 5g. Space-mean 500-mb chart, 0300 GCT, 17 December 1950.

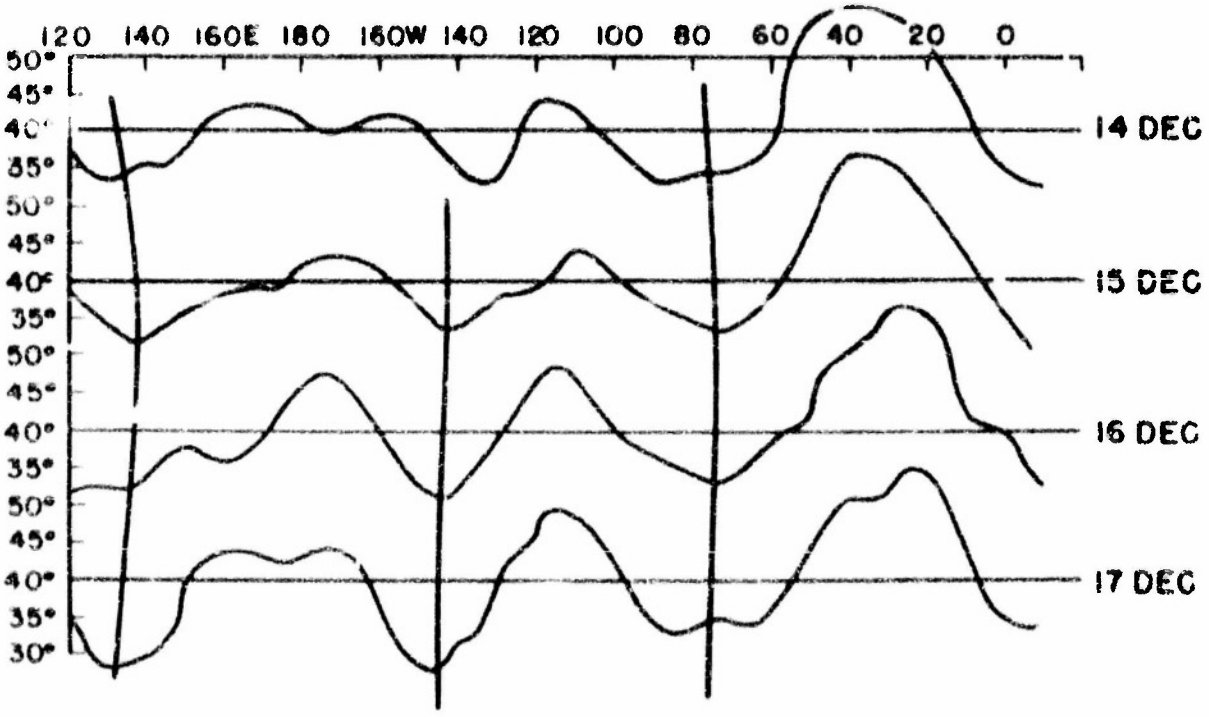

Quasi-vertical lines represent major trough positions

Figure 5h. Profile of the 10,400-ft contours at 500 mb, 14-17 December 1950.

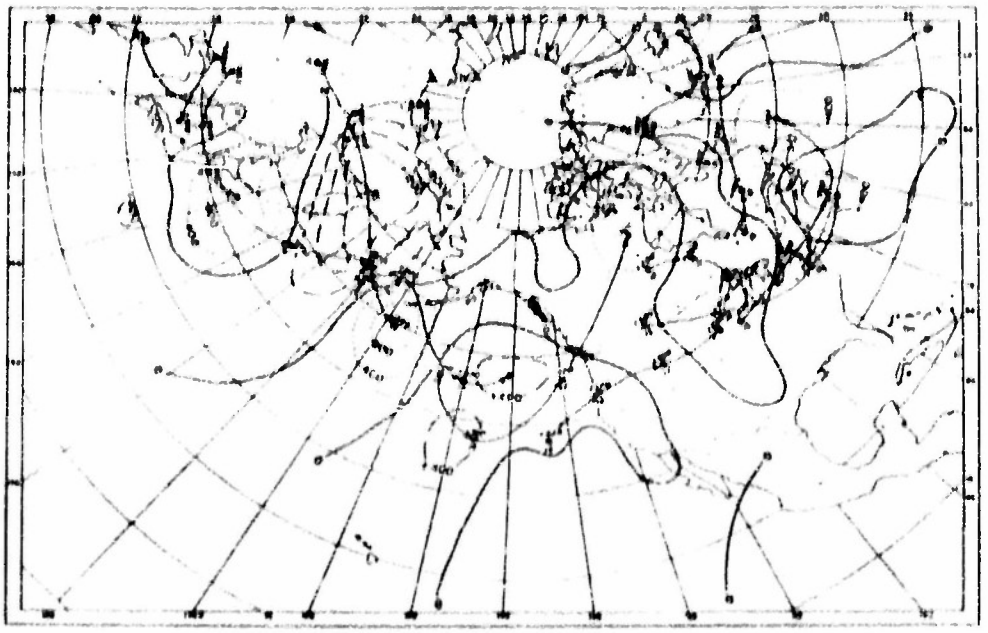

Figure 51. 24-hour 500-mb height changes, 0300 GCT, 17–18 December 1950, with trajectories of change centers.

are found at sea level as a result of the strong flow aloft. In general, families of wave cyclones can be observed in the West Atlantic and West Pacific, with a third family appearing in the East Pacific by 17 December 1950 (fig. 5f). In middle latitudes, where the upper long-wave pattern is found, under the major ridges the surface anticyclones are strong and the troughs and lows are feeble. Under the major troughs, particularly on their east sides, the reverse condition is found, i.e., strong cyclonic activity, and little or no anticyclonic activity.

2.7.1.4. The trajectories of the 24-hour height-change patterns at 500 mb (fig. 5l), follow the band of maximum wind, traveling north around the major ridges and south around the major troughs. The upper-flow pattern in this situation constitutes a stable steering pattern.

2.8.9. Retrogression of Long Waves. A continuous retrogression of long-wave troughs, in which the wave troughs are conserved, is a rare event. The usual type of retrogression takes place in a discontinuous fashion whereby a major trough weakens, accelerates eastward, and is transformed into a minor trough, while a major wave trough forms to the west of the former position of the old one. New major troughs are generally formed by the transformation of minor troughs into deep cold troughs. Since the old troughs are weakening and new ones developing during this process, it would be improper to attempt to apply equation (3) in a phase-velocity computation.

2.8.1. Equation (3) does indicate, however, the possibility of retrogression and therefore is useful in forecasting retrogression. When the actual wave length exceeds the stationary wave length, a shortening of the wave length is to be expected. There are two possibilities for this adjustment. The first is a retrogression, as described above. The second possibility is that of an increase in the wave number, i.e., the formation of a new major trough which is not compensated for by the disappearance of an old one, resulting in an increase in the number of major troughs in the circumpolar westerlies. It is not always possible to forecast which of these two possibilities will become an actuality.

2.8.2. Retrogression is seldom a localized phenomenon, but as a rule appears to occur as a series of retrogressions in several of the long waves. Examination of the periods of retrogression shows that retrogression generally begins in a quasi-stationary long-wave train when the stationary wave length shows a significant decrease. This can happen as a result of a decrease in zonal wind speed, or of a southward shift of the zonal westerlies.

8.8.3. Some characteristics of a retrogression regime are:—

a. Trajectories of 24-hour height-change patterns at 500 mb deviate from the band of maximum wind. New centers appear or existing ones rapidly increase in intensity.

b. Rapid intensification of surface cyclones to the west of existing major trough positions.

8.8.4.0. AN EXAMPLE OF THE RETROGRESSION PROCESS is shown on the maps for the period 6–8 November 1953. (See figs. 6a–f.) The 500-mb chart and space-mean chart for 6 November 1953 (see figs. 6a, 6c) show a long-wave pattern from Asia to the Rocky Mountains with major troughs in the western Pacific and extreme Western United States. The trough at 145–150°E has been quasi-

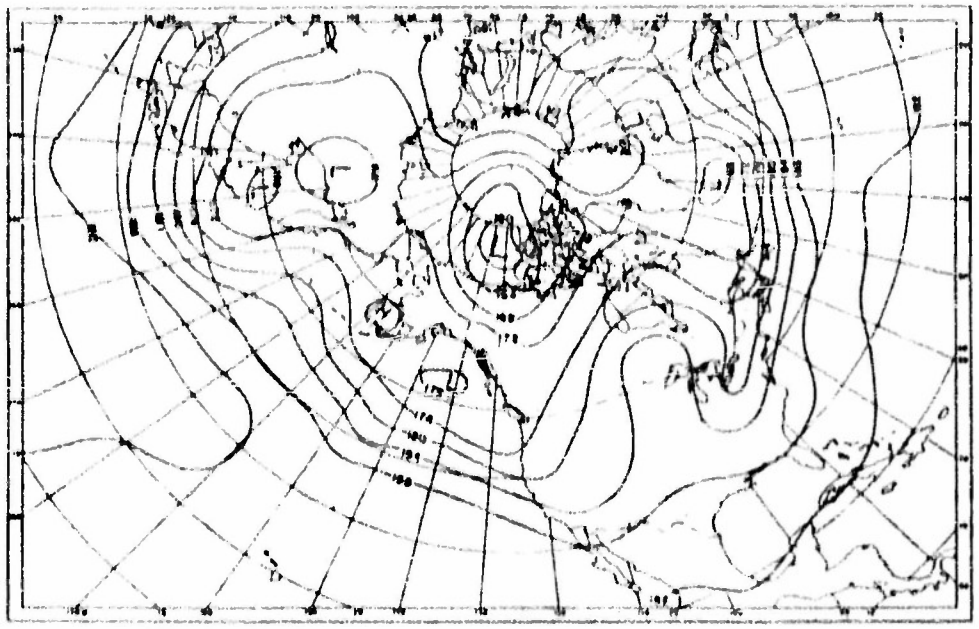

Figure 6a. 500-mb chart, 0300 GCT, 6 November 1953.

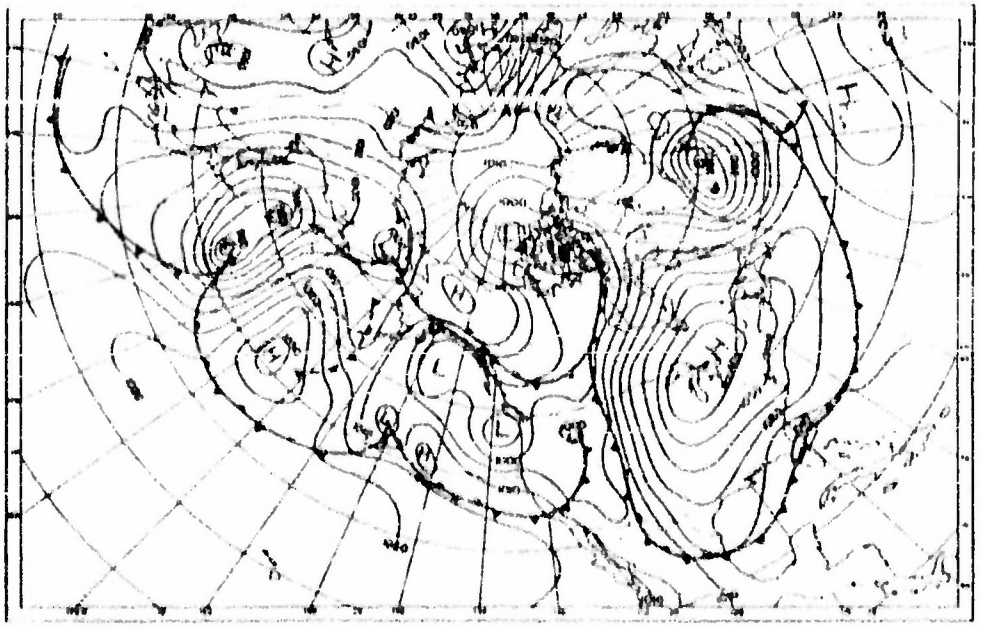

Figure 6b. Sea-level chart, 0030 GCT, 6 November 1953.

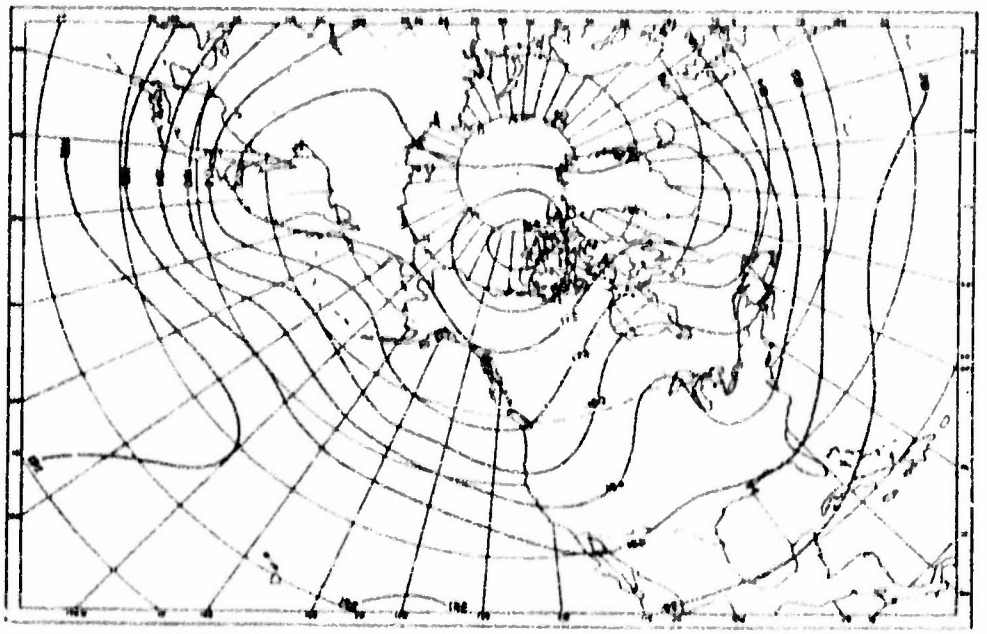

Figure 6c. Space-mean 500-mb chart, 0300 GCT, 6 November 1953.

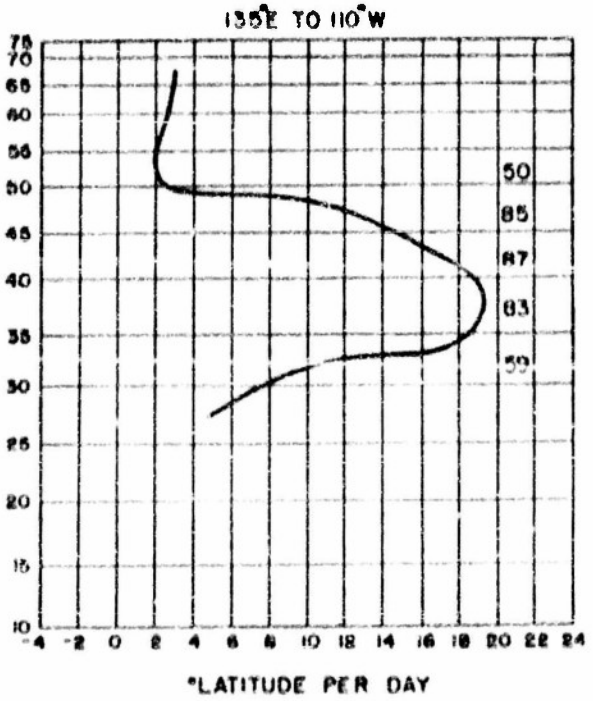

Figure 6d. Zonal wind profile and stationary wave lengths for 0300 GCT, 6 November 1953.

stationary at this position since 2 November 1953. Small-scale troughs have been moving through the trough and this regime continues throughout the example. In the eastern Pacific the major trough entering the U. S. on 6 November 1953 has been progressing slowly for several days. (Fig. 6i).

8.8.4.1. The stationary wave length for the Pacific sector obtained from the zonal wind profile (fig. 6d) is 83 long. deg. in the zone 35-40°N, which coincides closely with the position of the current westerlies on the 500-mb chart. The comparison of stationary and actual wave lengths then is L_s = 83°, L = 95°. (Note that if the value of 87° at 40-45°N were selected for L_s, the indication of retrogression would not be changed.) The indicated retrogression occurs quickly. The weak trough near 155°W on 6 November 1953 deepens rapidly (fig. 6a) and assumes the role of a slow moving major trough by 7 November 1953 (fig. 6e). Stationary wave lengths for 7 and 8 November 1953 were 83 and 82 long. deg. respectively for the zone 35-40°N. The old major trough loses its identity as it moves into the blocking situation over eastern North America (fig. 6g). The sea-level charts for 6-8 November 1953 (figs. 6b, 6f, 6h), clearly show the rapid change of weather regime over the eastern Pacific and western North America (e.g., strong anticyclogenesis along U. S. West Coast). The net amount of retrogression shown from 6 to 8 November 1953 amounts to 20 degrees at 500 mb.

8.8.4.2. The strong meridional flow pattern at 500 mb over North America eastward to Europe

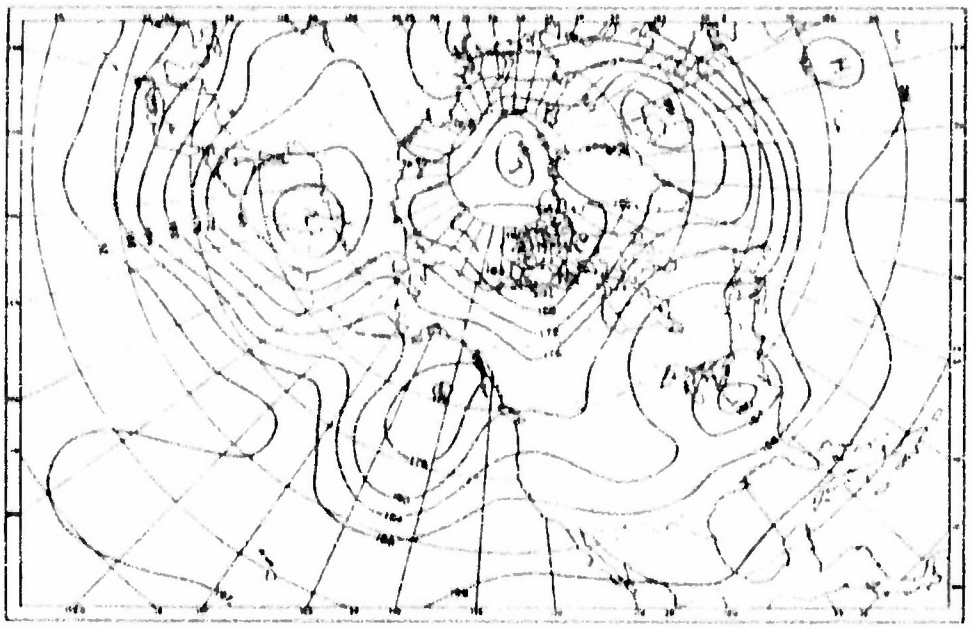

Figure 6e. 500-mb chart, 0300 GCT, 7 November 1953.

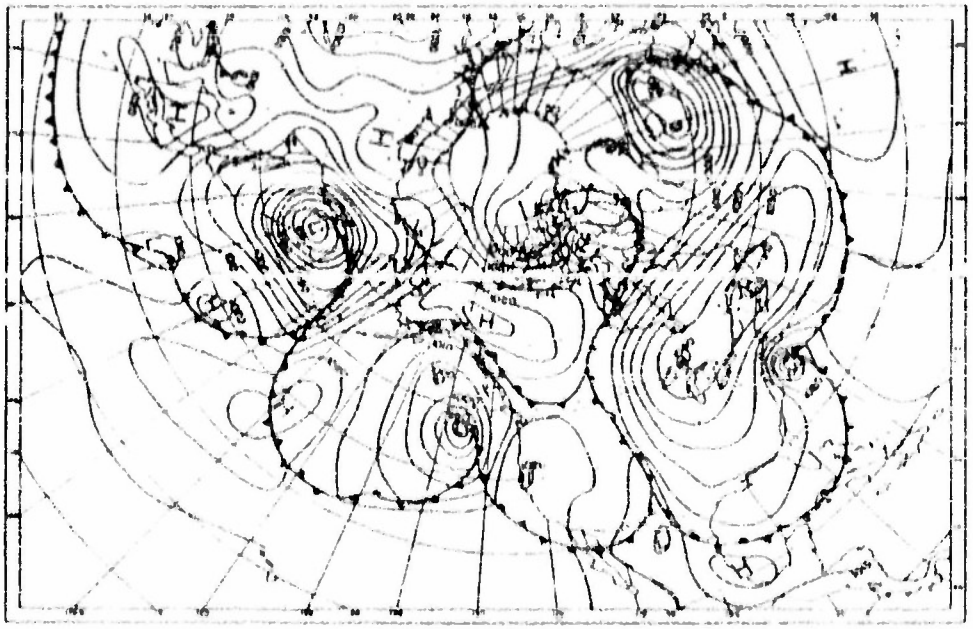

Figure 6f. Sea-level chart, 0030 GCT, 7 November 1953.

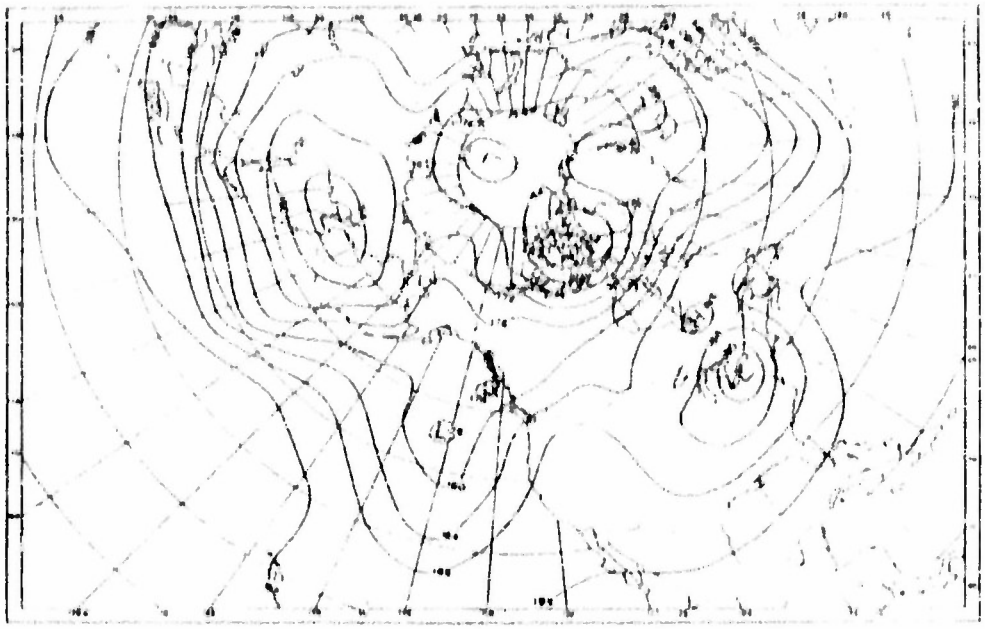

Figure 6g. 500-mb chart, 0300 GCT, 8 November 1953.

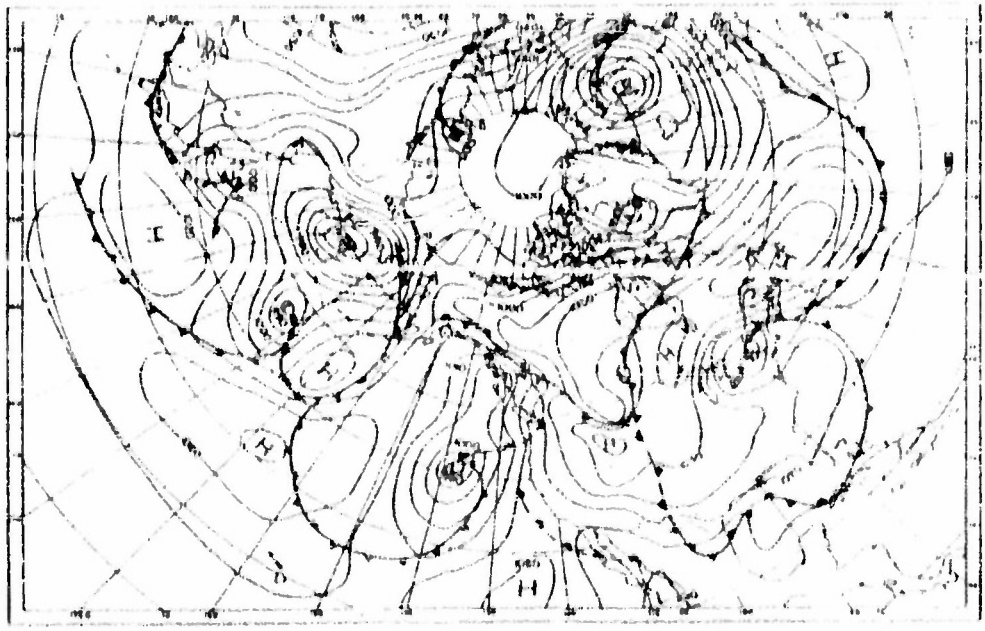

Figure 6h. Sea-level chart, 0030 GCT, 8 November 1953.

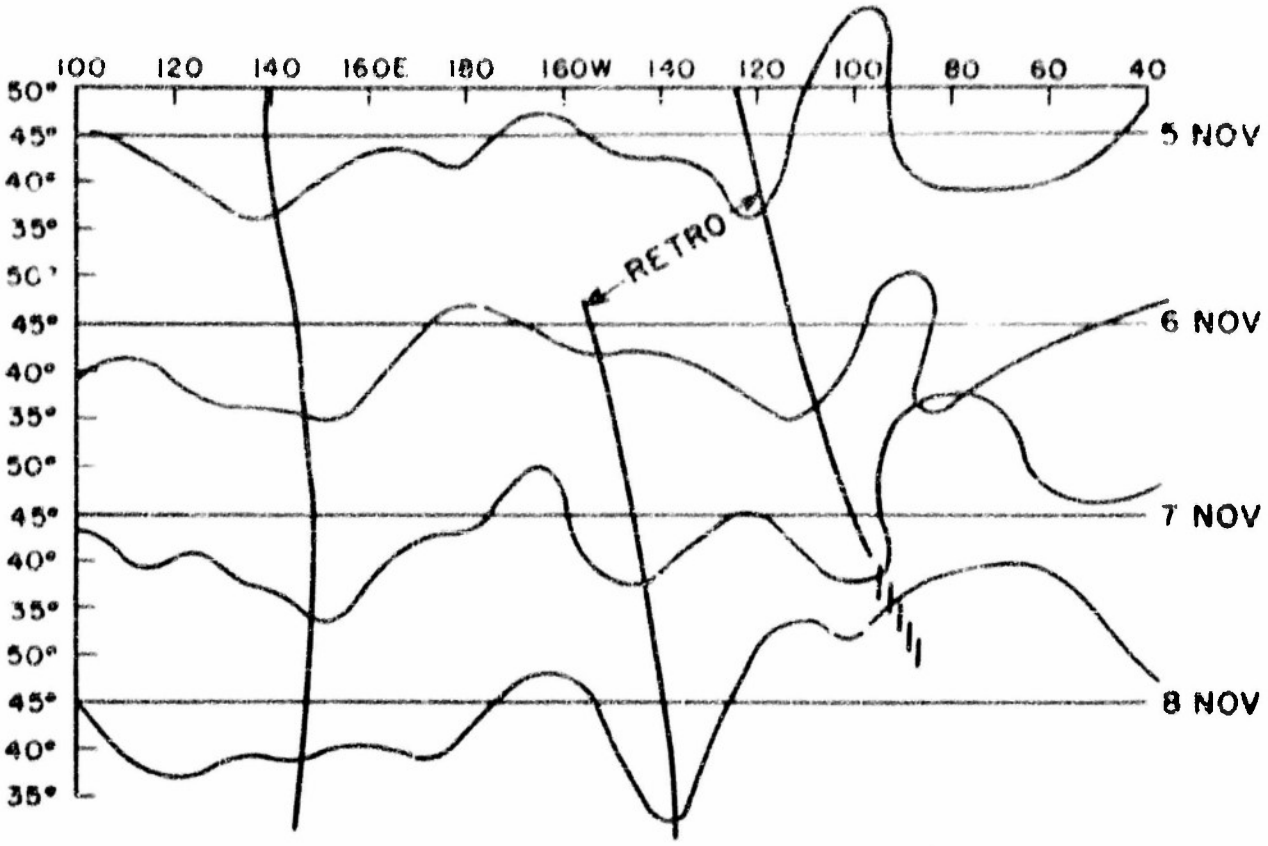

Figure 61. Profile of the 18,400-foot contour at 500 mb, 5–8 November 1955. Quasi-vertical lines represent major trough positions.

on 6–8 November 1953 is a good example of a flow pattern to which equation (3) should not be applied.

2.9. Increasing Wave Number. As mentioned above, when the actual wave length exceeds the stationary wave length another adjustment in the long-wave pattern which can occur is the formation of a new major trough which is not compensated for by the disappearance of an old trough. This development is often associated with retrogression. When a change of wave number is associated with retrogression, the old major trough progresses eastward with little or no weakening as the new trough develops. A general rule of some value is as follows: If L exceeds L_s by a small amount (e.g., 10 long. deg. or so), retrogression will occur. If L exceeds L_s by a larger amount, the wave number will increase. Numerous exceptions to this rule can be found. To forecast the exceptions close attention must be directed to intensity changes of the old trough.

Short-term constant absolute-vorticity trajectories (see Sect. IV) have been found of some value in determining intensity changes. The period of 23–27 September 1952 over eastern Atlantic and Eurasia illustrates a change in wave number associated with retrogression. (Example not reproduced.)

2.10. Decreasing Wave Number. A decrease in the number of major troughs in a long-wave pattern occurs in connection with rapidly increasing stationary wave lengths, usually as the westerlies are shifting toward the north. There are two possibilities for this decrease. One is the "cutting off" of a major trough as described in Section II *c*, par. 2.14.1–2.14.2. The other possibility is the marked filling of a trough such that it disappears or moves out as a minor trough. The trough in which this process occurs is usually one which is only a short distance (usually less than $L_s/2$) downstream from another major trough. A spectacular example of a decrease in wave number by filling up of a major trough took place 13–17 September 1952 in the eastern Atlantic. (Example not reproduced.)

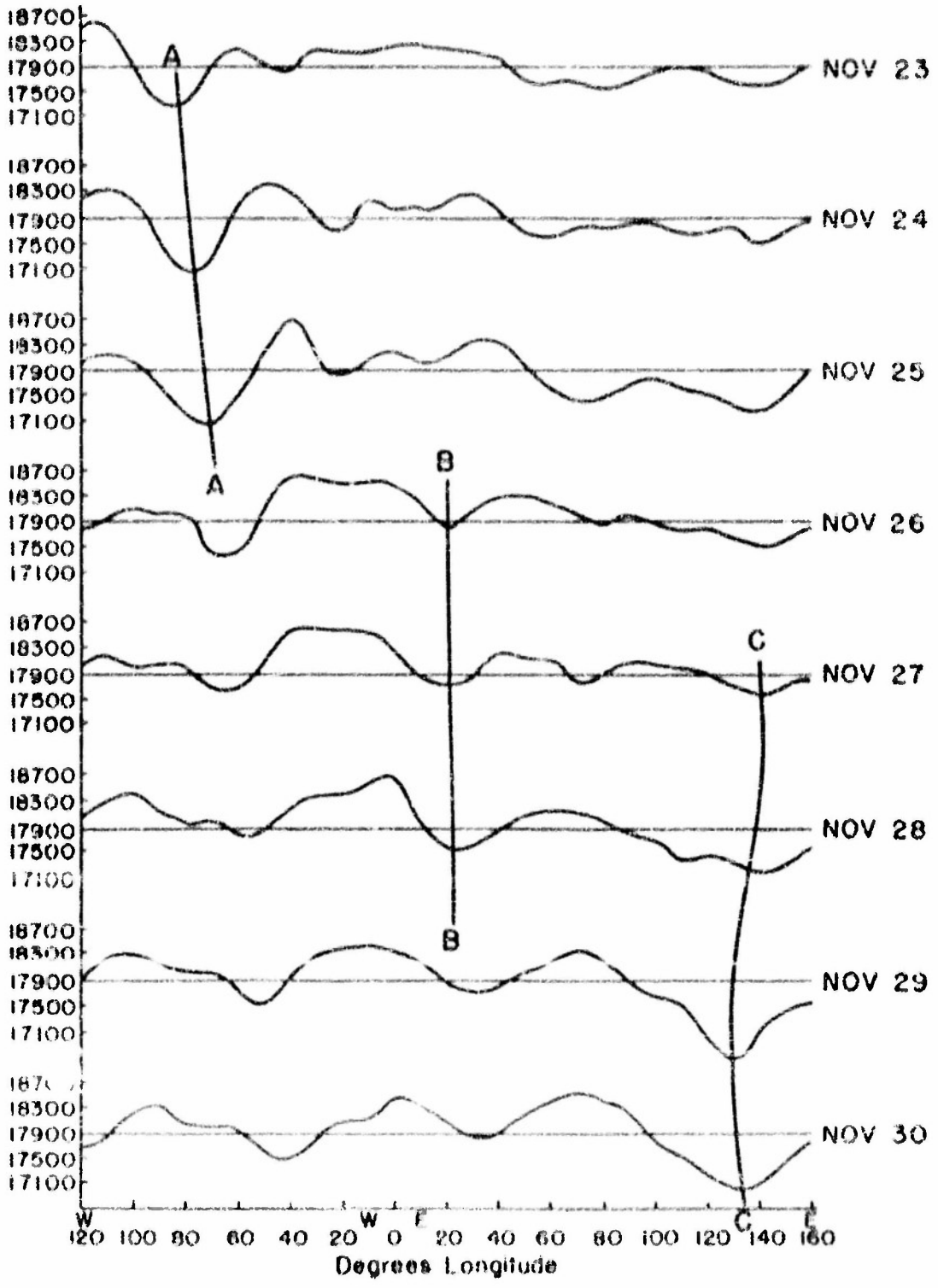

Figure 7. Profile of the average height in feet of the 500-mb surface between 40°N and 55°N, shown as a function of longitude, November 1945.

B. CHANGES OF AMPLITUDE OF THE LONG WAVES

2.11. Forecasting Amplitudes. Our ability to predict amplitude changes of the long waves is much less than our ability to forecast their motion. Their amplitudes are influenced by many complicated effects from features such as the longitudinal variations of amplitude and wave length (Rossby [29]), reinforcement or weakening of the pattern by large-scale mountain effects (Charney and Eliassen [5]), and local conversion of potential into kinetic energy (Charney, Fjörtoft and von Neumann [6]). There is little doubt that the systematic forecasting of amplitudes will have to await further research (see par. 2.16). However, a few processes can be recognized and used in a forecast.

2.12.0. Propagation of Amplitude Changes Downstream. Rossby [29], Yeh [35], Crossman [7], and Staff Members of the University of Chicago [33] have described a process in which a pronounced release of energy in a trough is followed in a very short time by formation and intensification of a wave pattern downstream. They ascribe this type of development to the theory that a "dispersion of energy" downstream takes place at a speed equal to the group velocity (i.e., approximately twice the speed of the zonal wind) of the wave pattern. Although the relationship between a release of kinetic energy in a trough and the following formation or intensification of the wave pattern, has been known empirically to forecasters for many years, the application to the atmosphere of the theory of the energy dispersion for forecasting changes of amplitude is still not well understood (see par. 2.12.3). Nonetheless, this application of the Rossby theory [29] has verified consistently enough to consider it a good forecasting tool.

2.12.1. Examples of this process of downstream propagation have been discussed by Crossman [7]. Figure 7, taken from his paper [7], shows one of them. On 23 November 1945, when the deepening of trough A was beginning, the downstream pattern was poorly defined. However, shortly after trough A began to deepen, the ridge to its east intensified. This was followed in succession by the formation of trough B, the formation of a ridge east of trough B, and the deepening of trough C. As shown by this example, the sequence of events which began with a deepening in North America continued until a strong deepening occurred north of Japan a few days later. Recently Carlin [17] published the results of another interesting case study of the process. A similar process but on 5-day mean charts, starting with a deepening in the Gulf of Alaska, has been described by Namias and Clapp [19].

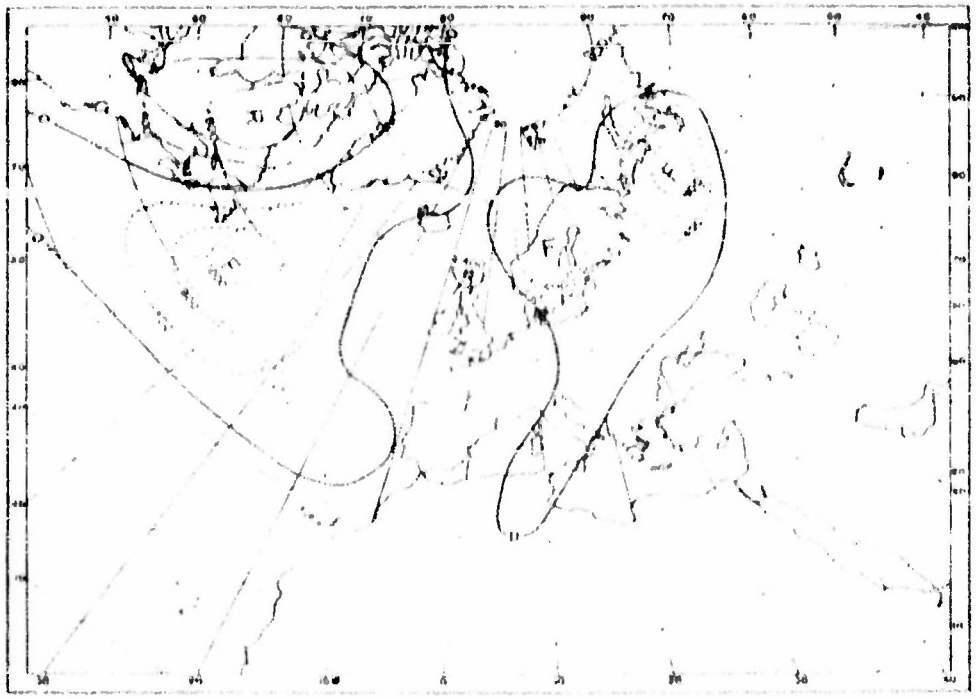

Figure 8a. 48-hr height changes at 500 mb, 0300 GCT, 1–3 October 1949.

8.18.2 An example from October 1949 is presented in figures 8a–g. Here as in the preceding example (fig. 7), when in a long-wave pattern a pronounced amplitude increase occurred in one section, similar amplitude increases subsequently were observed downstream. This particular situation was selected partly because a successful forecast of the amplitude changes in this series was made in the USAF Weather Central, Air Weather Service, from the above principle.

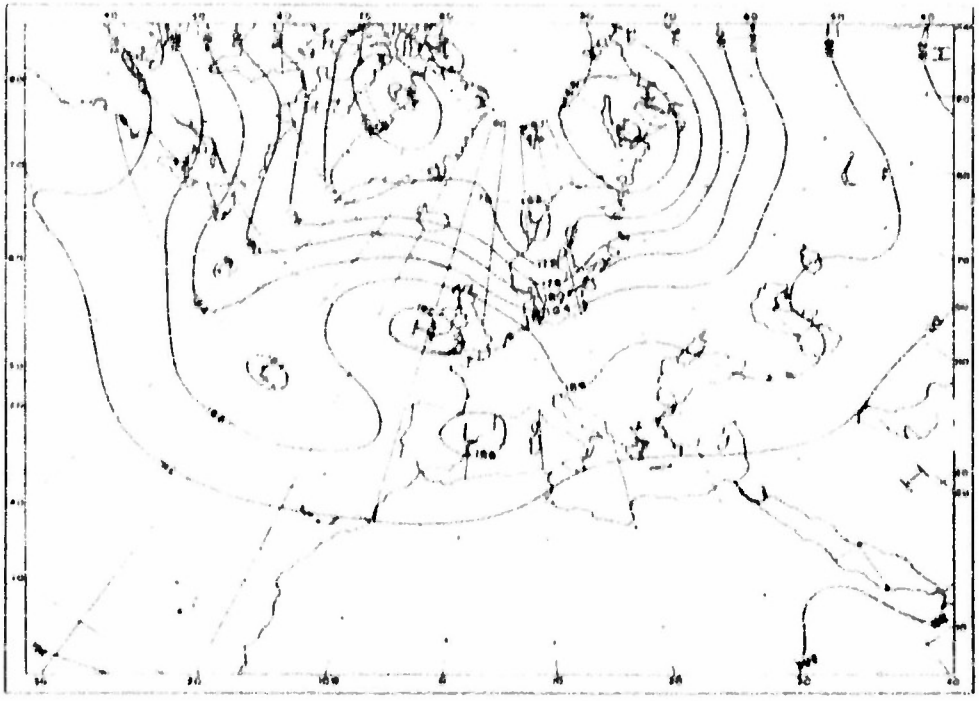

Figure 8b. 500-mb chart, 0300 GCT, 3 October 1949.

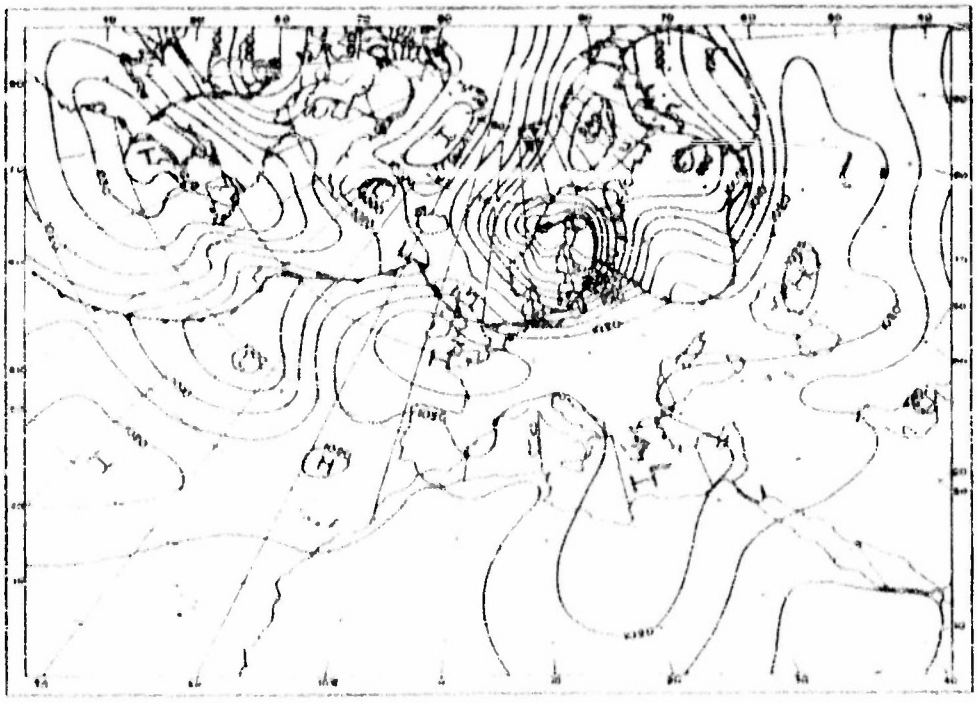

Figure 8c. Sea-level chart, 0630 GCT, 3 October 1949.

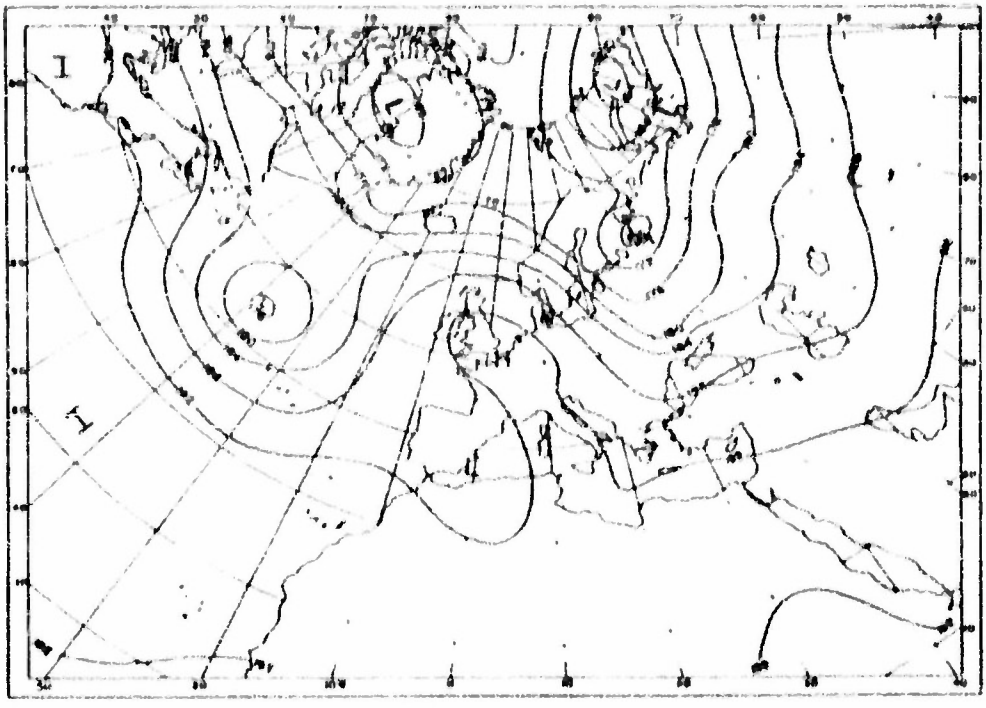

Figure 8d. 500-mb chart, 0300 GCT, 4 October 1949

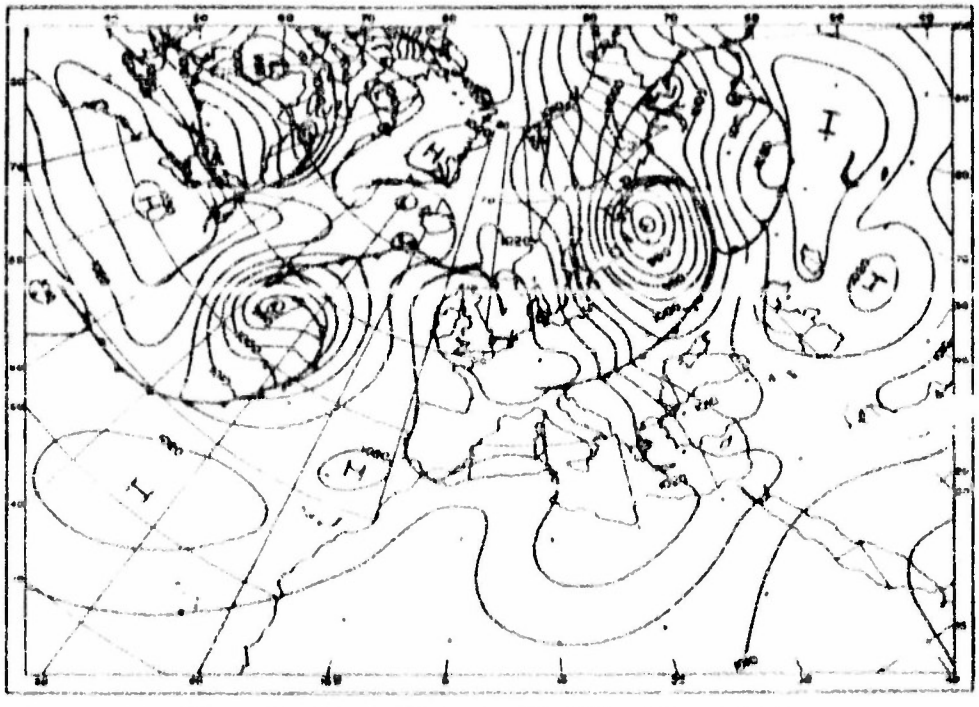

Figure 8e. Sea-level chart, 0630 GCT, 4 October 1949.

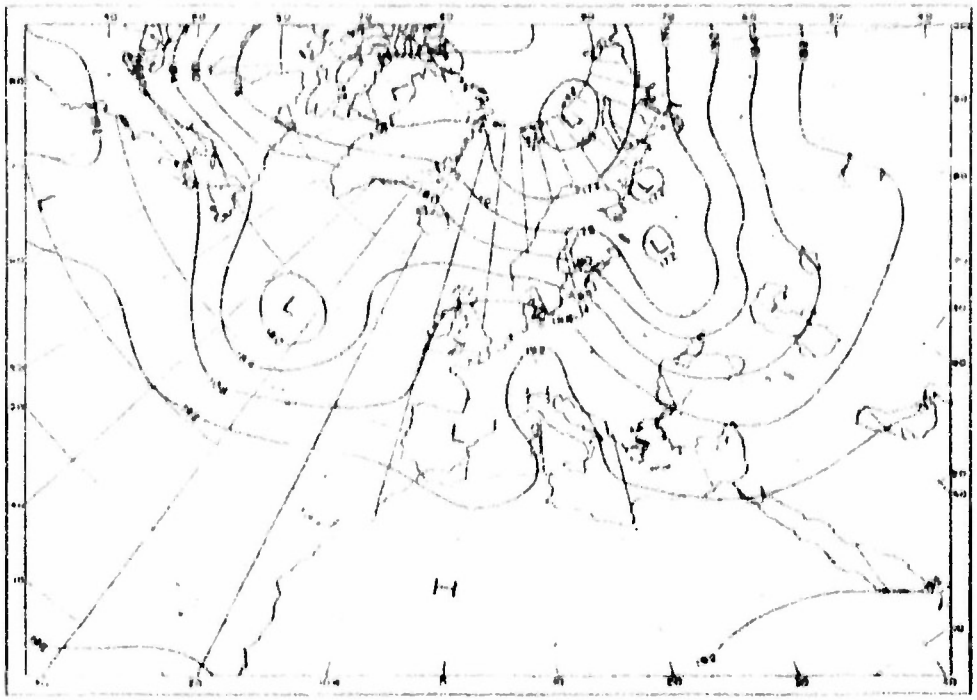

Figure 6f. 500-mb chart, 0300 GCT, 5 October 1949.

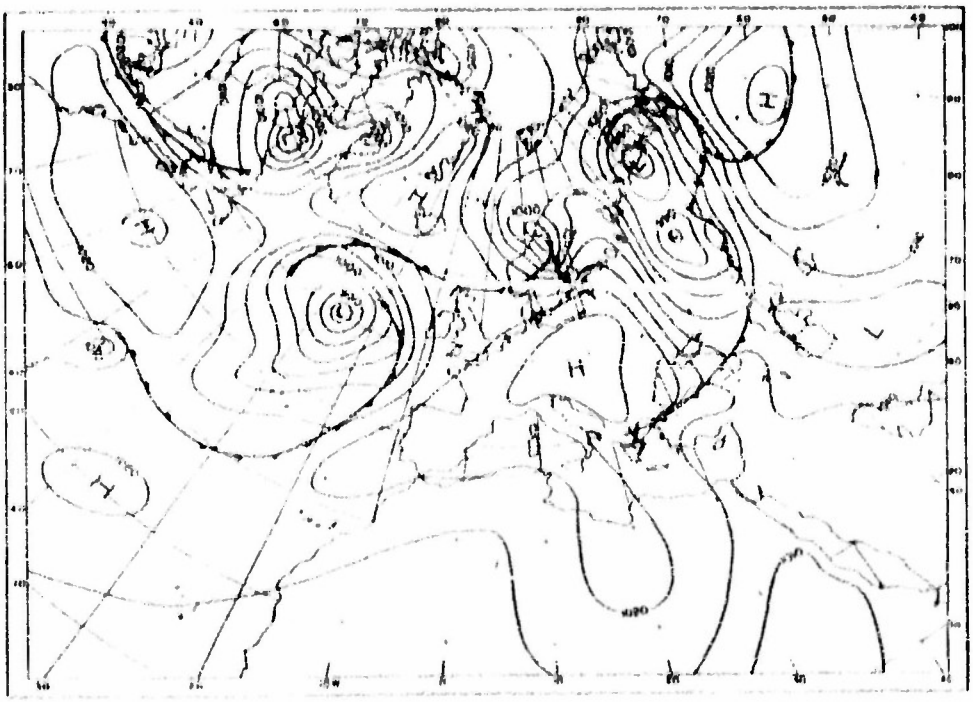

Figure 6g. Sea-level chart, 0630 GCT, 5 October 1949.

The 500-mb chart for 3 October 1949 (fig. 8b) shows a pronounced major trough over the Atlantic Ocean. Downstream from this trough is a strong zonal current which flows through a flat trough over Asia. The pattern over the western Atlantic and western North America is in an advanced stage of a pronounced amplitude increase, as shown by the 48-hour change patterns (fig. 8a). This is indicated particularly by the northerly position of the rise area over Labrador with respect to the fall area in the Atlantic. The deepening in the Atlantic continued until 4 October 1949 (figs. 8d, 8e) when the major trough there attained its greatest depth. However, by this time a strong deepening had already begun over northwest Russia. By 5 October a deep cold-trough was completely developed over western Russia (fig. 8f). The formation of an intense cold low at the surface between Moscow and Sverdlovsk during this period should also be noted (fig. 8g).

The increase of amplitudes did not stop with the formation of the deep trough over western Russia, but was observed even farther downstream. From 5 to 7 October 1949, a pronounced deepening of the next major trough, in the western Pacific, was observed.

2.12.4. The THEORY OF THE DOWNSTREAM DISPERSION OF ENERGY assumes that the atmosphere is essentially barotropic. However, there are other sound theoretical and observational reasons to believe that *baroclinic effects* must be included to explain intensification of the waves. Baroclinic effects are evidenced in the fact that for several decades forecasters have found it possible to anticipate certain places and times when the amplitude of the upper-flow pattern will increase or decrease by noting areas of indicated advection of warm and cold air. This is observed when, in the middle troposphere, the isotherm pattern is out of phase with the streamline pattern. As an example, in the case of a north-south asymmetric streamline trough, where the isotherm trough is found west of the streamline trough, an increase in cyclonic vorticity can be expected in the streamline trough. Similarly for ridges, if an isotherm ridge is found west of a symmetric north-south streamline ridge, an increase in anticyclonic relative vorticity can be expected in the streamline ridge. In other words, cold-air advection is associated with falling pressures, and warm-air advection with rising pressures in the middle and upper troposphere.

The effects of the baroclinity can, to a certain extent, be considered separately from the barotropic changes, at times reinforcing and at times opposing them. There is also the possibility that barotropic effects will change the circulation patterns so as to influence the conditions under which potential energy is converted into kinetic energy, i.e., "trigger" the baroclinic effects. In recent years these baroclinic effects have been incorporated into numerical forecasts made by the use of an electronic computer [6], [37], [38].

E. CHANGES OF SHAPE OF THE LONG WAVES

2.13. Blocking. Changes in the general appearance or shape of the long waves, as distinguished from changes of position, usually occur as the structure of the basic zonal current changes. One type of change is observed when a split of the zonal current occurs. If the split affects a relatively limited area, a blocking situation is said to exist, as described by Namias [18], Rex [25], and others. Within the area affected by the blocking, the long-wave pattern no longer exists. If the split of the zonal current occurs on a hemispheric scale, as described by Cressman [9], separate wave patterns can be found in each current, having different wave lengths and phase relationships. (See par. 2.14.3.)

2.14.0. Cut-off Low. A process is commonly observed in which the northern part of a major trough fills up or accelerates eastward, while the southern part of the trough shows little change in position and intensity. By this process a closed cold low (aloft) is formed in relatively low latitudes. This type of development has been called the *cutting-off* process, with the formation of a *cut-off low*. A considerable amount of literature exists on this subject, e.g., [15] [36].

2.14.1. A striking example of the formation of a cut-off low (fig. 9), is given by Palmén [21]. On 1 November 1946, a pronounced major trough was found along western North America. The subsequent formation of the cold low over New Mexico was accompanied by a notable weakening and eastward acceleration of the northern part of the trough. This process involves the advection of high values of the absolute vorticity out of the high latitudes into the low latitudes. At the same time the low forms in the south, the trough in the north weakens

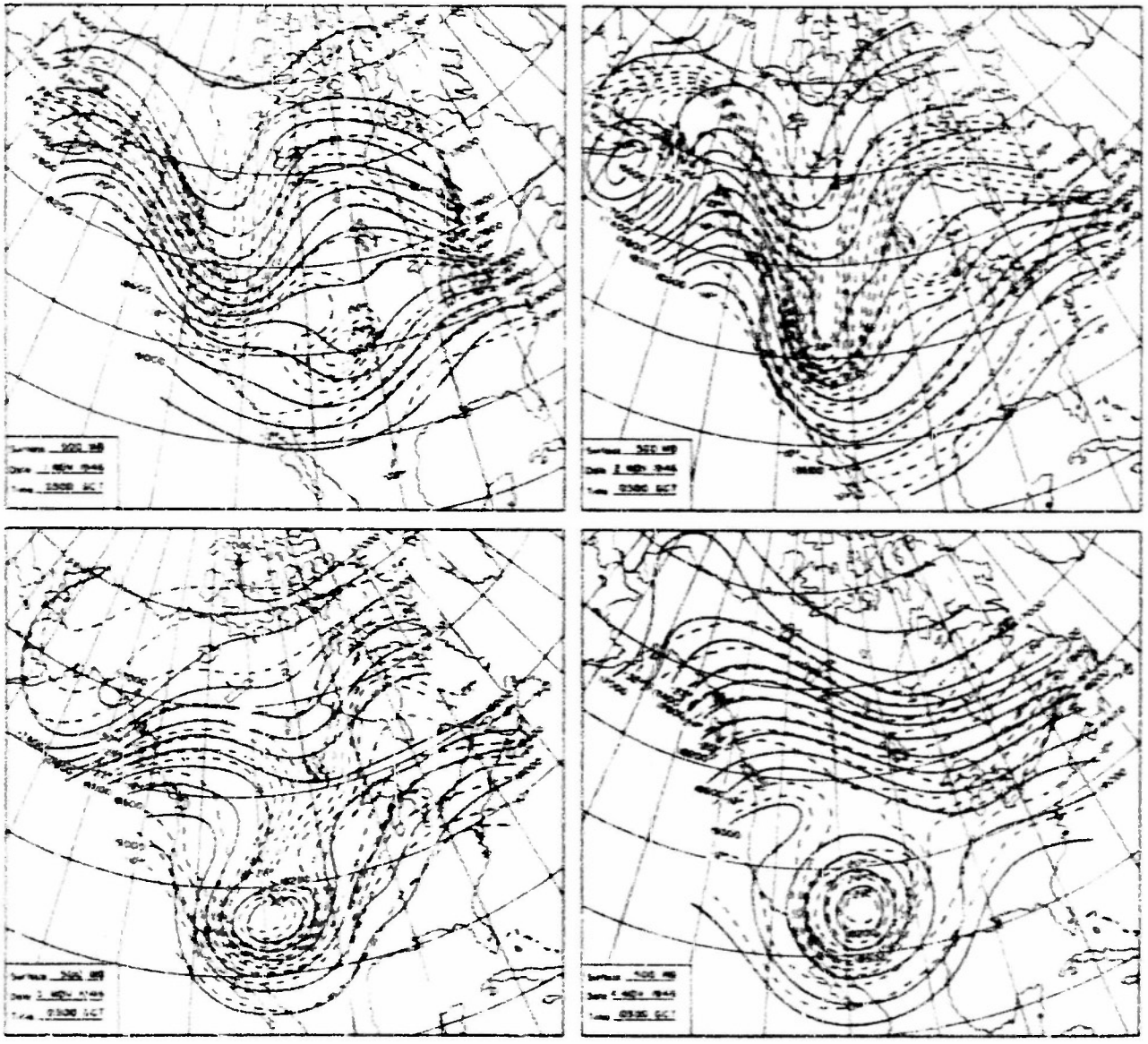

Figure 9. 500-mb charts, 1-4 November 1946. (After Palmén).

2.14.2. It has been observed (Cressman [7]) that there is a distinct tendency for several of these cut-off lows to form at about the same time at widely separated places on the hemisphere. This can be associated with the splitting of a zonal current on a hemispheric scale. These lows mark the trough positions of the long-wave pattern in the southern current. If the splitting and cyclone formation occur in relatively low latitudes, e.g., about 40°N, the lower-latitude current would be most intense at or above 200 mb, and would be largely obscured at 700 mb. At 700 mb the cut-off lows would then appear to be isolated cyclones without any connecting current.

2.14.3. The development of a split in the zonal current of westerlies, either over a small area or on a hemispheric scale will radically alter the structure of the long waves. At present it is not possible to forecast such a split with any amount of accuracy until it is actually under way. A possible line of attack on this problem, based on theoretical work by Rossby [30], has been published by Rex [25] but has not yet been thoroughly tested. (See also the suggestions in par. 2.16.)

F. REMARKS ON LIMITATIONS AND APPLICATION

2.15.0. Orographic Influences. The question often arises as to whether or not certain parts of the long-wave pattern can be considered as "key" features, their location being fixed by low-level solenoid fields or by terrain. Several excellent papers bearing on this subject have been written by Bolli [1], Wilkins [34], Stewart [32], Charney and Eliassen [5], and Bolin [2]. They have demonstrated that the larger relief features of the earth, in particular the Andes, the Rocky Mountains and the Himalayan-Central Asiatic plateaus tend to "anchor" ridges in the upper-wind field in the longitudes corresponding to the regions of high surface elevation. The dimensions of the trough-and-ridge pattern downstream depend on the stationary wave length. Wilkins indicated that the Central Asian plateaus produce the most pronounced topographical effect in the northern hemisphere; and that if the westerlies are found at low enough latitudes to impinge on the west side of the plateau, the ridge shift to the north is extremely dependable. If the westerlies are found at higher latitudes, the effect of the plateau is still important but not quite so dependable.

2.15.1. The influence of the Rocky Mountains is somewhat less strong than that of the Asian plateaus. When the maximum zonal flow is found in relatively low latitudes, persistent cold troughs are occasionally found over the Rockies. However, if the maximum westerlies are found in higher latitudes, the presence of an upper ridge is more dependable. The effect of the Asian plateaus is often strong enough to disrupt the long-wave pattern in its vicinity, whereas the effect of the Rockies is most often expressed in a lack of symmetry of the long wave in that area. This will be observed as a temporary influence in fixing the upper ridge over the Rockies while the major troughs to the east and to the west move along.

2.15.2. THE GREATEST DIFFICULTY AND MOST IMPORTANT LIMITATION IN THE APPLICATION OF LONG-WAVE TECHNIQUES IN DAILY FORECASTING ARISES FROM THE FACT THAT THE ATMOSPHERE DOES NOT ALWAYS PRESENT A PICTURE OF A WELL-DEFINED ZONAL CURRENT HAVING QUASI-SINUSOIDAL PERTURBATIONS. The first step in the forecast routine, then, is to select the area on the upper-air charts where the actual flow pattern approaches this model—an area where there is a well-defined zonal current containing major troughs and ridges. For other areas, which may be characterized by blocking, for example, long-wave techniques are not appropriate, and other techniques to be discussed in other parts of this manual must be used.

2.15.3. For example, the 500-mb chart for 2 April 1951 (fig. 10), contains a strong belt of westerlies at mid-latitudes from central Asia through the western and central Pacific. There is one major trough over the east coast of Asia and another one at about 165°W. In the eastern Pacific the westerlies split into two distinct currents, one at high and another at low latitudes. Both branches are very weak over western North America. A blocking situation, as defined by Rex [25], exists over this area. In this case a computation of trough motion can be made successfully on the major trough at 165°W; but due to the large alteration in the pattern downstream from this area, long-wave techniques should not be applied to the low off California or to the trough over eastern North America. *The methods of forecasting long-wave motion, as described previously, should be considered as a tool to be used on certain recognizable types of flow patterns.* Their indiscriminate use on all types of flow patterns will lead to a large percentage of failures.

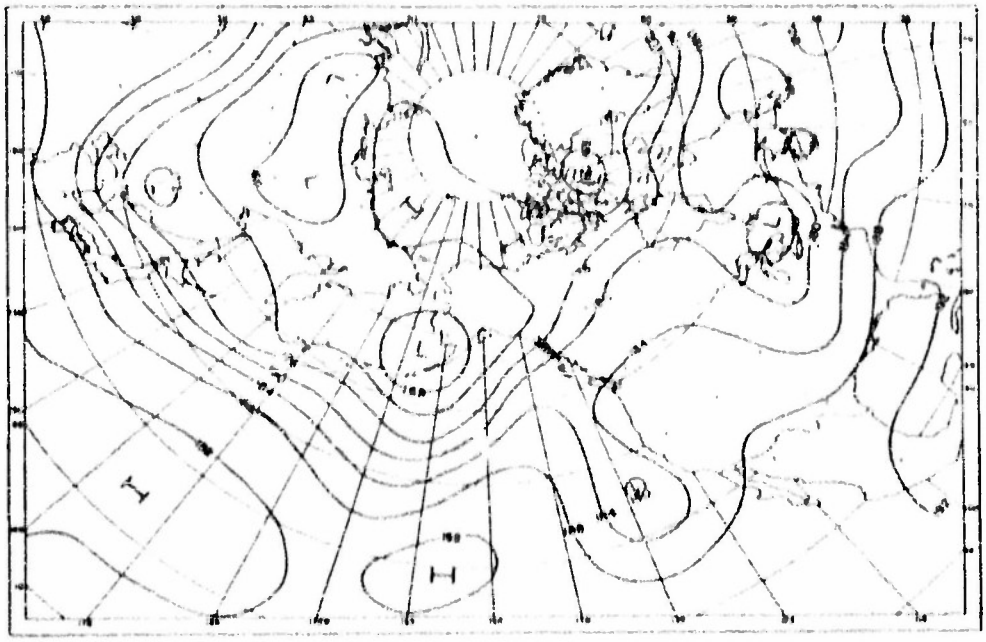

Figure 10. 500-mb chart, 1500 GCT, 2 April 1951.

G. NEW TECHNIQUES IN LONG-WAVE FORECASTING

2.16.0 Trend of Research. The rapid developments in the field of numerical weather prediction during the last few years strongly suggest that in the near future forecasts of large-scale flow patterns (and small-scale patterns) will be prepared objectively either by the use of an electronic computer, or by graphical means. Fjörtoft [11] has done the pioneer work in graphical methods of numerical prediction, realizing that the services and/or products of an expensive electronic computer would not be available to many forecasting stations for several years.

2.16.1. Fjörtoft Method. Section IIIA (par. 3.1–3.2 below) discusses the use of this graphical method in the forecasting of the smaller scale flow patterns. In April 1954, Fjörtoft demonstrated at Headquarters, AWS, an extension of this method, whereby larger-scale (long-wave) flow patterns could be forecast for periods of 24 to 48 hours. If this method is as successful as preliminary tests have indicated, those parts of the herein discussed long-wave forecasting technique which are based on the use of the Rossby equation will be outmoded and replaced by more objective graphical methods. A brief description of the procedure for Fjörtoft's new method follows. Detachments with sufficient facilities to experiment with this new approach are encouraged to do so.

2.16.2. Forecasting the Long-Waves by the Fjörtoft Graphical Technique. Forecasting of the long-wave pattern by graphical means consists of mapping the absolute vorticity of the long-wave pattern and advecting it in a suitable flow field. The advective-field is obtained by constructing a space-mean chart of the original $\bar{Z}$-chart (see para. 2.4.0), called a $\bar{\bar{Z}}$ ("double Zee-bar") chart, using a grid size of 720 nautical miles, and adding to the $\bar{\bar{Z}}$ a field which accounts for the grid length, change of Coriolis parameter with latitude, and map projection. The graphical steps are similar to those used in constructing a $\bar{Z}$-chart. (See Appendix V.) The additional field, M_s, is added graphically to the $\bar{Z}$ chart. M_s is invariant with time, and can therefore be computed once and for all for the map projection used. The following values are for the polar stereographic projection and grid size of 720 nautical miles:

24.5°N	200 feet	54.5°N	800 feet
37.5°N	400 feet	62.0°N	1000 feet
46.0°N	600 feet	70.5°N	1200 feet

Note that this field is an east to west flow-field which results in reducing and distorting the $\bar{Z}$-field. (M-field is negligible for the small grid used in obtaining the $\bar{Z}$-flow, and therefore has been neglected

(Continued on page 41)

Section III

MOTION OF THE SMALLER-SCALE SYSTEMS IN MID-TROPOSPHERE

A. THE USE OF VORTICITY CHARTS

3.0. Relative Vorticity Charts. Charts of the relative vorticity at 500 mb have proved useful in the forecasting of the smaller-scale flow patterns in mid-troposphere during a trial period of two years. The principle involved is one which has been well established by trials in numerical prediction, namely that the majority of the changes in these patterns observed in mid-troposphere can be accounted for by horizontal advection of absolute vorticity. For short time periods and small-scale systems it is also true that the relative vorticity in mid-troposphere can be treated as a relatively conservative property. Due to the presence of vertical shear in the atmosphere, this can be true in the average for one level only. Cressman [10] found in two different situations that lines of absolute vorticity (lines of relative vorticity also, to a good approximation) moved with the following percentages of the wind speed normal to the lines:

Constant-pressure surface (mb)	700	500	300
8–7 January 1958			
Mean movement of lines (per cent of normal wind speed)	121	79	50
Standard deviation (percentage)	24	19	12
Standard deviation of mean (percentage)	3.7	3.0	1.8
Number of measurements	43	43	43
16–20 June 1958			
Mean movement of lines (per cent of normal wind speed)	113	74	49
Standard deviation (percentage)	30	18	05
Standard deviation of mean (percentage)	4.9	2.6	3.0
Number of measurements	34	34	34

From the above data it can be concluded that the vorticity lines move with approximately the speed of the wind normal to them at 60% mb, or with approximately 80 percent of the 500-mb normal wind speed. A recommended procedure for using the principle follows:

a. *Analysis of the vorticity chart* can be accomplished quickly by graphical methods. With reference to the grid of figure 3, the relative vorticity, ζ_r can be written as

$$\zeta_r = \frac{4g}{fd^2}(Z_B - \bar{Z}_B),$$

where g is the acceleration of gravity, f is the Coriolis parameter, d is the grid size (distance from E to A), and $\bar{Z}_B = (Z_A + Z_B + Z_C + Z_D)/4$. If the original 500-mb chart is subtracted graphically from the space-mean ($\bar{Z}$) of the same chart (see Appendix), the resulting quantity ($\bar{Z} - Z$), is used as a representation of the relative vorticity.

b. *The movement of the relative vorticity* or ($\bar{Z} - Z$) lines is then given by 80 percent of the component of the 500-mb wind normal to the vorticity lines. Using the geostrophic approximation to the 500-mb wind, the motion of the ($\bar{Z} - Z$) lines can be calculated from their intersections with the 500-mb contours (Z lines) with the aid of a geostrophic wind scale. However, the only difference between the Z lines and the $\bar{Z}$ lines is the vorticity pattern ($\bar{Z} - Z$), which cannot advect itself. It follows therefore that the vorticity lines can also be advected with 80 percent of the wind component on the $\bar{Z}$ chart normal to the vorticity lines. It is customary, therefore, to copy the vorticity pattern ($\bar{Z} - Z$) on the space-mean ($\bar{Z}$) chart, and to compute the speed of the vorticity lines from their intersections with the $\bar{Z}$ lines. This is illustrated in figure 11. The speed of the ($\bar{Z} - Z$) line normal to

itself is obtained by using the geostrophic wind scale on the distance S_n in example (a). If the eastward speed of the vorticity line is desired, the geostrophic wind scale should be applied to the distance S_e, as in example (b). The advantages of using the $\bar{Z}$ lines to compute the motion of the $(\bar{Z} - Z)$ lines are: (1) the two sets of lines are as a rule more perpendicular to each other than would be the case if the Z lines were used, and (2) the $\bar{Z}$ pattern changes more slowly with time than the Z pattern.

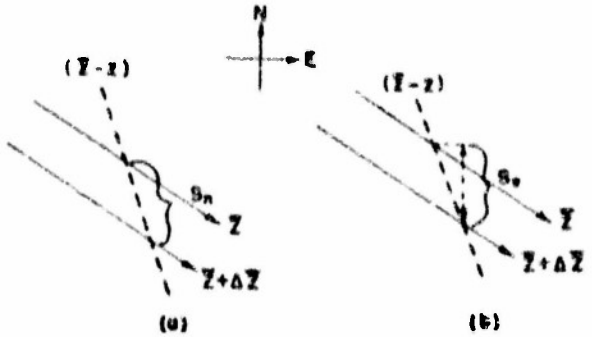

Figure 11. Schematic diagrams of advection of vorticity lines.

c. *Computations of the movement of the* $(\bar{Z} - Z)$ *lines* at map time can then be entered on the chart. Since the $(\bar{Z} - Z)$ lines characterise certain features of the flow pattern on the 500-mb (Z) chart, such as troughs and ridges, highs and lows, these features will be moving with speeds similar to those computed for the $(\bar{Z} - Z)$ lines. The use of the speed computed at map time for a time interval extending into the future is of course subject to changes in the $\bar{Z}$ chart. However, the $\bar{Z}$ chart is relatively stable, changing only slightly during most 24-hour periods, and to a good approximation the $(\bar{Z} - Z)$ lines can be visualised as moving along through a stable $\bar{Z}$ pattern for periods up to 24 hours. Movements in the $\bar{Z}$ pattern reflect movements of the long-wave pattern, and in the case of stationary long waves the $\bar{Z}$ pattern can be considered stationary for periods in excess of 24 hours.

3.1.0. An Example. An example of a computation with the aid of a vorticity chart is shown in figures 12*a*–c. Computations of the eastward motion of the $(\bar{Z} - Z)$ lines associated with a 500-mb trough and low are entered on the space-mean and vorticity chart. The following conclusions can be drawn from the computations in this example:

(1) The vorticity lines on the west side of the trough are moving eastward more rapidly than those on the east side of the trough, implying a sharpening up of the trough.

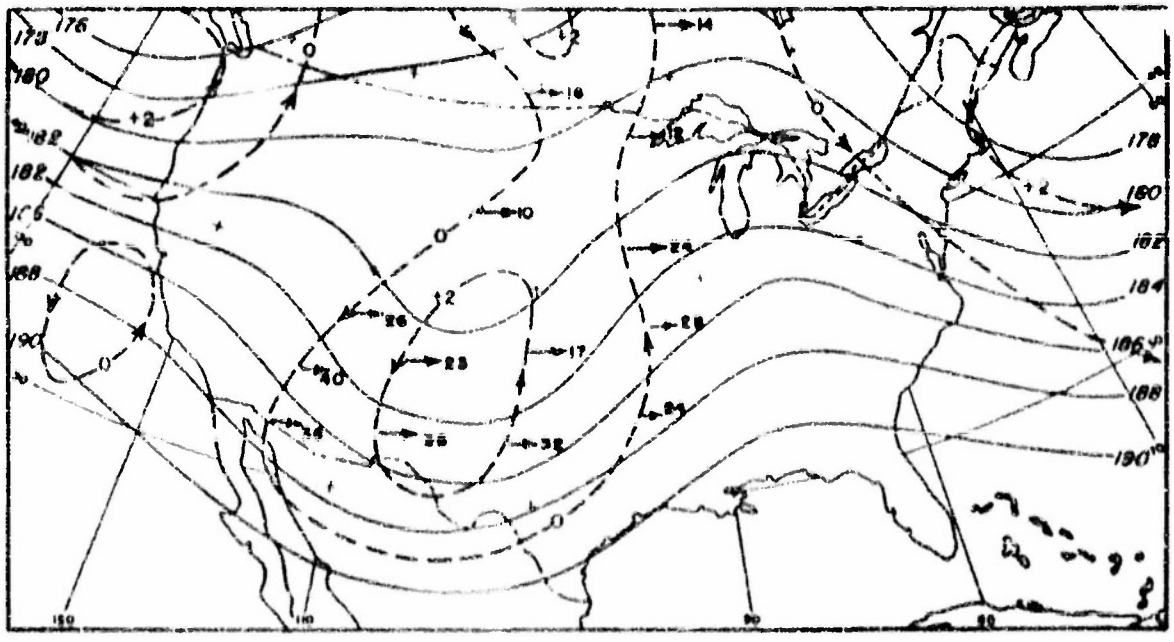

Solid lines are contours of space-mean chart. Dashed lines are relative vorticity ($\bar{Z} - Z$) lines. Motion indicated is in knots.

Figure 12a. Advection of vorticity lines using space-mean chart at 500 mb, 0300GCT, 18 March 1952.

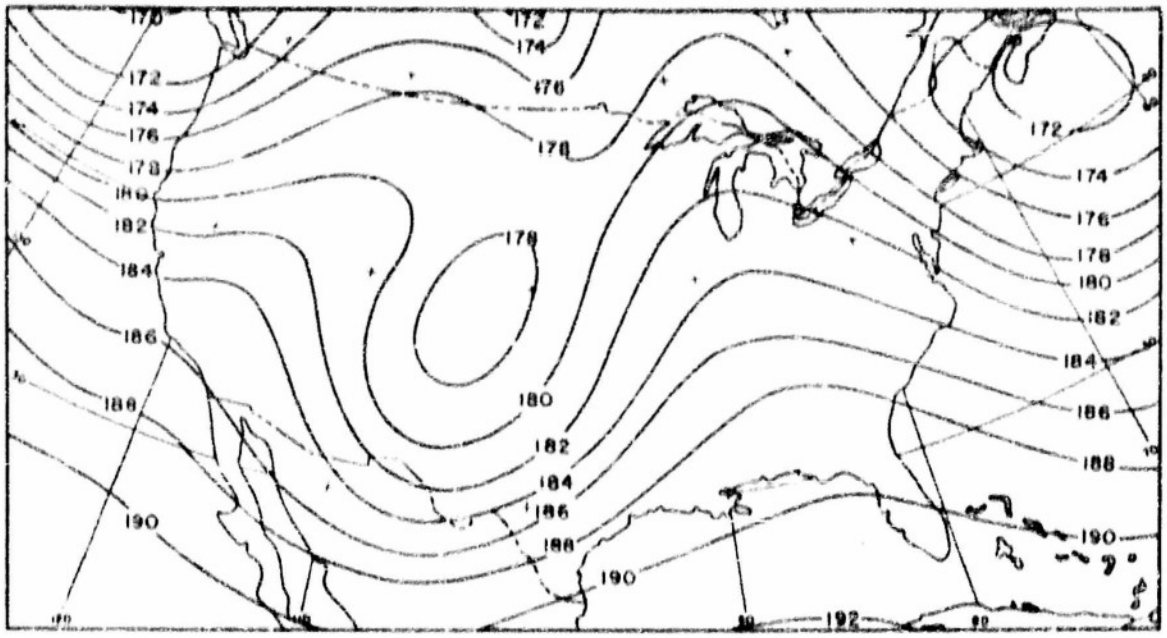

Figure 12b. 500-mb chart, 0300 GCT, 18 March 1952.

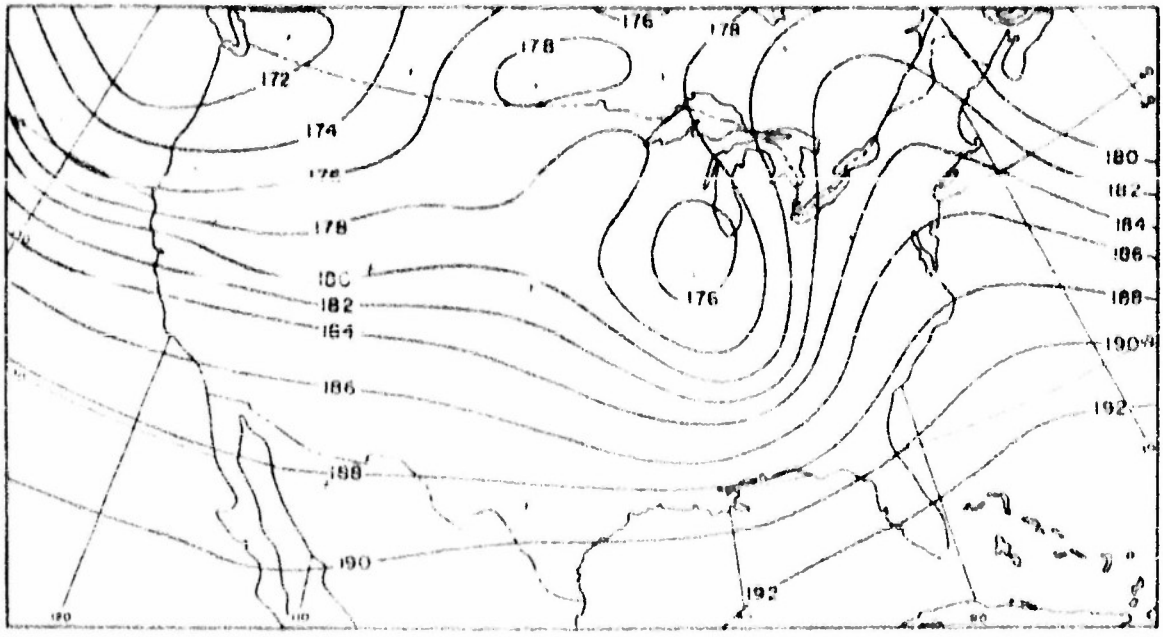

Figure 12c. 500-mb chart, 0300 GCT, 19 March 1952.

(2) The average of the computations between 30° and 40°N, where the main part of the trough is found is 20 knots (toward the east). The average of the computations between 40° and 50°N is 15 knots. This difference in eastward speed at the different latitudes indicates a certain amount of rotation of the trough.

3.1.1. The 500-mb charts for computation time and for 24 hours later are reproduced to show how the computations verified.

3.2. Errors. Some of the errors arising from the simplifying assumptions underlying this method are mentioned below:

a. Graphical or procedural errors made in the process of obtaining the Z and $(Z - \bar{Z})$ charts. These can be eliminated as the analyst becomes experienced in the operation.

b. Errors in the vorticity analysis due to the large grid size used. These result in underestimation of relative vorticities associated with strong horizontal shear. They show up most often by leading to overestimation of the motion of anticyclones or ridges when strong horizontal shear exists south of the jet. Nothing can be done about this type of error except to watch for it, as the grid size is fixed within narrow limits by many considerations.

c. Errors in the vorticity analysis arising from errors in the original 500-mb analysis. With the large grid size used, these are usually not serious unless gross errors exist in the original 500-mb analysis.

d. Errors in the forecast due to the operation of nonbarotropic processes. These affect the intensity of the vorticity patterns, but seldom have a significant influence on the speed computations for short periods.

B. MOTION OF TROUGHS AND RIDGES FROM THE PETTERSSEN EQUATION

3.3.0. The Equation. Pettersson [23] has arrived at the equation for the motion of troughs and ridges,

$$C = \frac{U - (L/2\pi)^2 \beta}{1 + (L/2\pi B)^2},$$

where:

C = speed of the trough or ridge line,
U = wind speed at the trough or ridge line in the core of the jet,
β = northward variation of the Coriolis parameter,
L = wave length, and
B = half-width of jet.

3.3.1. The troughs and ridges of the long-wave pattern are usually determined by points of minimum and maximum latitude of the contours on an upper-air chart. They may also be determined by maximum curvature of the contours. However, when minor troughs and ridges are superimposed on the long-wave pattern, the resulting analysis is complex. The minor systems are always characterized by maximum streamline curvature. The formula given by Pettersson was derived to apply to troughs (or ridges) having maximum curvature of streamlines, and not necessarily running through points of minimum (or maximum) latitude of the contours. In view of this fact, the following suggestions can be offered for its application:

a. If there are no minor troughs or ridges superimposed on the long-wave pattern, the equation may be applied to the long waves, since the major troughs and ridges are then characterized by maximum curvature of the contours.

b. If minor systems are superimposed on the long-wave pattern, the computations should be made on the superimposed minor troughs or ridges, and not on the major systems. For example, if there is a wide trough (as is often the case with a slowly moving major trough) the streamlines and isotherms should be carefully inspected in the area of the trough for indications of minor troughs. The isotherms will often offer a good clue. If such a minor trough is found it is the computation on this that should be attempted.

3.3.2. Tests. It has been found [16] that the Pettersson equation gives the best results when applied on the 500-mb charts. This alone does not necessarily mean that 500 mb is near the mean level of non-divergence, but rather that the total effect of all the terms assumed negligible in the derivation is least near 500 mb. This is shown by the average algebraic (systematic) error (troughs

and ridges included together) from a sample of 100 computations:*

Surface	Average algebraic (systematic) error (long. deg./day)
700 mb	−3.8
500 mb	+2.3
300 mb	+13.7

5.3.2.1. The various parameters used in the equation should be measured as follows:

a. The wave length, L, is determined as twice the distance from the trough (ridge) to be computed and the upstream ridge (trough) in the jet stream. Again, the necessity for careful selection of the proper systems to be used must be emphasized. For example, when computing the motion of a trough, one should go upstream along the jet and choose as the ridge line the first line of maximum anticyclonic curvature of the streamlines. The use of flat major ridges should not be attempted.

b. The latitude is that of the trough (ridge) line at the jet stream.

c. The core speed, U is the maximum wind speed of the jet at the trough (ridge) line, determined as a best estimate from observed and gradient winds.

d. The half width, B, along the trough (ridge) line, is the mean of the distances from the core of the jet to the points north and south of the jet where the wind speed first drops to a value of $U/2$. It is usually profitable to draw isotachs to obtain U and B.

e. The 24-hour displacement is given along a line perpendicular to the trough (ridge) line, and passing through the jet stream at the starting position. This is usually a distance along a west-east axis.

5.3.2.2. The best results will be obtained if the troughs (ridges) to be computed are selected under the following conditions:

a. *Adequate upper-wind data are necessary.*

b. Only cases should be selected *where the streamlines have a well-defined sinusoidal pattern from the trough (ridge) in question for a distance of $L/8$ upstream.* Symmetry of wave lengths up and downstream about the trough (ridge) is not required.

c. *A simple and fairly symmetric velocity profile along the trough (ridge) line is necessary.* If the velocity profile along the trough or ridge line is complex, with more than one maximum of speed, or with a notable lack of symmetry, large errors may result.

5.3.2.3. A test of 157 troughs and ridges by Johannessen and Crossman [16] has indicated that the following corrections should be applied to the results of the computations:

a. Deduct one longitude degree per day from each computation of trough speed.

b. Deduct three longitude degrees per day from the computed motion of each ridge east of the Rocky Mountains.

c. Deduct 5° per day from the computed motion of each ridge over the Rockies.

5.3.2.4. A further test by Johannessen and Crossman on a new sample of 50 cases was made. Here, the corrections indicated above were applied to the computations. The results are summarized in the following table:

No. of cases	50
Mean observed speed (long. deg./day)	9.4
Mean absolute error of computed speed (long. deg./day)	2.8
Mean error of an extrapolation forecast (long. deg./day)	5.5

5.3.3. Conclusions. It can be seen from the above results that the equation of Petterssen gives good results when the troughs and ridges to be computed are selected carefully, and when adequate data are available. The strict data requirements for this type of computation limit its effective use to the area of the United States, and possibly western Europe, where good data are available. There is no real conflict between the equations of Petterssen and Rossby, inasmuch as each is useful under certain specified conditions, and for certain purposes, as described earlier. The Rossby equation is suitable where the data are not so complete, i.e., over oceanic areas as well as over land, but will not give such a detailed forecast as the Petterssen equation, giving only the *long*-wave motions. The Petterssen equation may be regarded as a more accurate extension of Rossby's work, applicable where refined data permit its use.

* See Appendix for nomogram for solution of the equation.

Section IV

CONSTANT ABSOLUTE-VORTICITY TRAJECTORIES

4.0. Definition. The horizontal trajectory taken by an air parcel when its absolute vorticity is conserved (i.e., the relative vorticity changes only when the Coriolis parameter is changed) is defined as a *Constant Absolute-Vorticity Trajectory* (CAVT). These trajectories are computed from the same form of the vorticity equation as is used in deriving the long-wave equation.

4.1. Relation to Long-Wave Techniques. Since constant absolute-vorticity trajectories and the long-wave forecasting techniques are based on the same principle, they usually give similar results when applied to a forecast problem. However, the computation of individual trajectories can be made in more complicated patterns than those to which the long-wave techniques can be applied, particularly in the irregular patterns where wave length can hardly be defined. The basic *theory* of constant absolute-vorticity trajectories has been summarized by Rossby [28].

4.2. Choice of Level. Again the question of the vertical shear present in the westerlies must be considered. It is evident that in the atmosphere wave speed and wave-length are relatively constant with height, whereas the wind speed increases with height. The same reasoning applies here as was used in the application of equation (3) for the long waves. Since the mean level of non-divergence is near the 600-mb surface, the wind speeds at 600 mb should be applicable. In a comprehensive study of trajectories, Fultz [12] indicated that the 15,000-foot winds (about 600 mb) were probably the most suitable for use in the computations.

Assuming the wind generally increases with height, and the axes of the troughs and ridges are essentially vertical above 700 mb, this result means that the level of non-divergence and the best verification of the trajectories is to be found somewhere above 10,000 feet. In view of the work of Fultz and Namias and Clapp [20] approximately 600 mb seems to be the level from which winds should be selected for trajectory computation. In practice, however, these winds are estimated by selecting the initial point for computation at 500 mb and deducting one-fifth from the 500-mb wind speed. This is justified by the fact that the direction of the winds at 600 mb varies only very slightly from that at 500 mb in the pronounced currents where trajectories are to be computed (see para 4.3b below); and by the fact that in moderate or strong tropospheric currents the wind speed at 600 mb averages very close to 80% of the speed at 500 mb.

4.3. Selection of Initial Point for Computation of Constant-Vorticity Trajectories. This is the step upon which success or failure of the results often depends. The conditions for its selection are as follows:

a. The horizontal shear at the initial point should be zero. This condition is necessary because in the computations the relative vorticity is assumed to be due entirely to the curvature of the streamlines. The vorticity chart described in Section IIIA is frequently useful in determining this condition.

b. The winds at the point selected should be situated in a well-defined current, and should be at least 25 knots in speed. This is necessary since the wind speed is assumed to be constant in the trajectory computations. If a well-defined current is used the possibility of its decay during the forecast period is at a minimum.

c. The limitations of the computation methods generally available restrict the points of the trajectory computations to inflection points of the streamlines. This condition together with the first two conditions can then be combined to say that

the initial point for a computation should be selected in the center of and at an inflection point of a well-defined current.

Several computation methods have been published. Most methods involve a certain amount of error arising from various simplifying assumptions which are made. The use of tables or slide rules constructed for trajectories on a flat earth gives fairly accurate computations for middle latitudes for periods up to 36 hours. Special computers or correction graphs should be used for high latitudes and longer periods [13] [14]. It is found that the flow of air in the atmosphere differs from constant-vorticity paths more than the approximate computations do. This does not lessen the desirability of starting from accurate computations.

A mechanical differential analyser ("wiggle-wagon") has been constructed by H. B. Wobus which plots accurate constant-vorticity trajectories for a spherical earth directly on a map, but this apparatus is not generally available. The TABLES given in AWSTR 105–90 were computed with the aid of this computer and are recommended as being the most accurate available and the most convenient for use.

4.4.0. Methods of Using Constant-Vorticity Trajectories. There are several. The first and most direct method is to plot trajectories from as many starting points as possible and then to use the winds interpolated from the trajectories for the forecast time in the preparation of a prognostic chart. In verifying the results it is generally found that the wind direction will verify more closely than the wind speed. This can be explained partly by the fact that the wave length of the trajectory will verify better than the amplitude and partly by the fact that on any upper-air chart wind speed varies more rapidly in the horizontal than wind direction.

4.4.1. AN EXAMPLE of this procedure is given in figure 13. Due to the restrictions governing selection of the starting points, only six or seven trajectories could be computed from this map. Only four of these remained on the map for a 36-hour period. It can be seen that these four trajectories are not enough to yield sufficient information to draw a prognostic chart; but they do give forecast winds with which a prognostic chart, when constructed, should be made to agree.

4.4.2. ANOTHER USE of the trajectories is illustrated in the same figure. The times at which the trajectories pass points of maximum and minimum latitude fix forecasts of ridge- and trough-line positions at those times, giving a measure of ridge and trough movement.

It should be noted that in the above example there was a good flow of westerlies across the map. Similarly successful verifications will not be observed if the forecast trajectories run through a

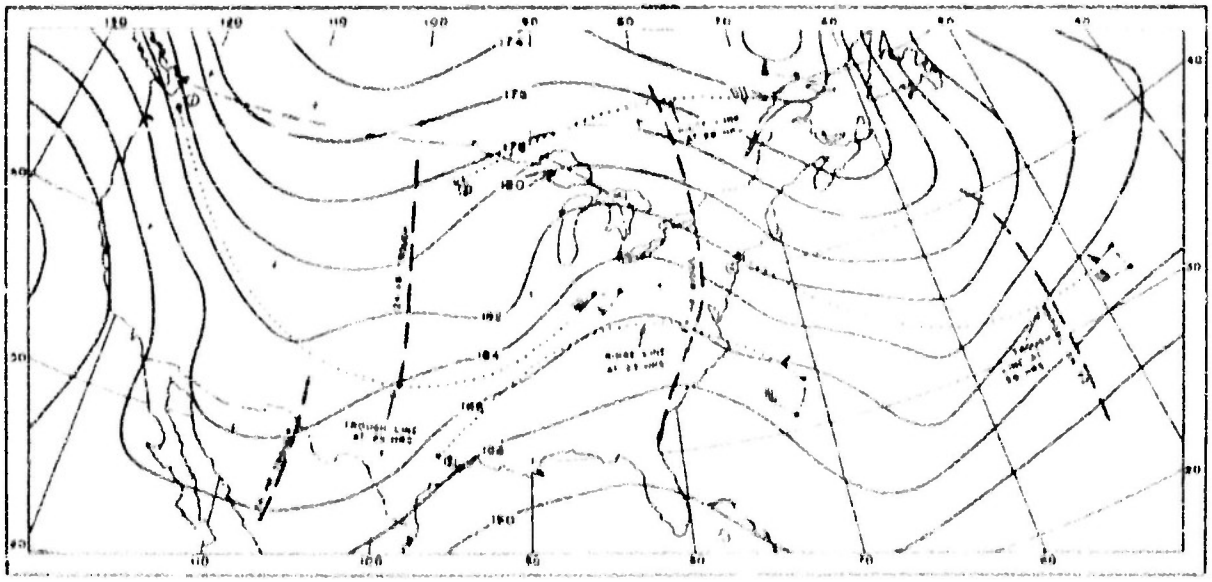

Computed constant absolute-vorticity trajectories for 36-hr periods are shown by dotted lines. Forecast winds are indicated by solid shafts and verifying winds by dashed shafts. Trough- and ridge-line points on trajectories are indicated by thin arrows, along with time of trough- and ridge-line positions. 36-hour actual trough and ridge lines are indicated by heavy dashed lines.

Figure 13. 500-mb chart, 1500 GCT, 27 March 1951.

large area of stagnant circulation or an area of blocking. If forecast trajectories from a well-developed current enter and pass through such an area on several successive maps, one should expect a penetration of the westerly current into the stagnant or blocking area. This penetration will occur in approximately the same place as indicated by the trajectories, but at a slower rate.

4.5. Applicability. Since the computation of these trajectories is based on the same principle as the long-wave techniques described earlier, it is to be expected that approximately similar results can be obtained from the use of both methods. However, it would not be proper to conclude that one or the other method is superfluous. Rather, the computation of a number of constant-vorticity trajectories on a map provides a convenient check on the results from the long-wave analysis. One is never so confident in a forecast by any method that a check is not desirable. Also, as mentioned previously, constant-vorticity trajectories can be applied somewhat more widely than the long-wave methods.

(Continued from page 33)

in Section III A.) A representation of the absolute-vorticity-field is now obtained by subtracting the $\bar{Z}$-field from the $\bar{Z} + M_s$-field. The advection of this vorticity field by 100% (tentative value) of the $\bar{Z} + M_s$-field indicates the motion of the long-wave features. Advection is computed for 24 and/or 48 hours. This advection is based on the assumption that the $\bar{Z}$-field varies very slowly with time. The height-profile chart (para. 2.5) of a $\bar{Z}$-contour could be used as a check on this assumption. An approximation of the forecast long-wave pattern is obtained by adding the $\bar{Z} + M_s$-field to the forecast vorticity pattern, $Z - (\bar{Z} + M_s)$.

The motion of troughs and ridges of the long-wave pattern are determined by a comparison of the magnitudes of the $\bar{Z}$- and M_s-flow fields: *stationary*, $\bar{Z}$-field equals M_s-field; *retrogression*, $\bar{Z}$-field less than M_s-field; *progression*, $\bar{Z}$-field greater than M_s-field.

Appendix

A1.0. Computations of Stationary Wave Length and Zonal Wind Speed.* After the sector for computation has been designated, the height and temperature of the 500-mb surface can be tabulated separately at the intersections of the latitude circles (every 5°) and the meridians (every 10°). These data then yield, after averaging along the latitude circles, the average height and temperature of the 500-mb surface for each 5° latitude circle within the sector selected. An example of the height tabulation for sector 20°W–135°W in figure 4a is illustrated in figure A1.

A1.1. The equation of state and the hydrostatic equation, when combined, give the result that

$$\Delta h_{850} - \Delta h_{500} = 18\Delta T_{850}$$

where ΔT_{850} is the difference in Celsius (Centigrade) degrees between the average temperature along a latitude circle and the average temperature along a second latitude circle 5° farther south (northward decrease of temperature giving positive values). The quantities Δh_{500} and Δh_{850} are the differences of the average heights in feet along the first and second latitude circles at 500 mb and 850 mb

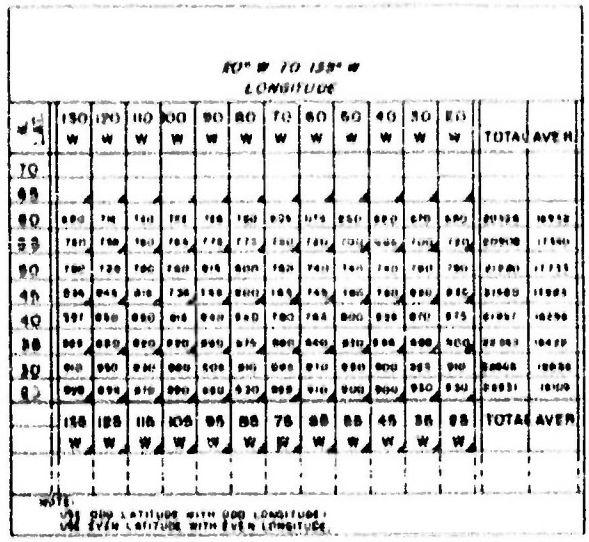

Heights of 500-mb surface at appropriate latitude and longitude intersections and total of the heights for given latitude are plotted as abbreviated figures. (e. g. 680 represents 18,680 ft; 20320 represents 203,260 ft). Tabulated height data is taken from figure 4a.

Figure A1. Height tabulation scheme used at USAF Weather Central in computing Zonal Wind Components and Stationary Wave Length.

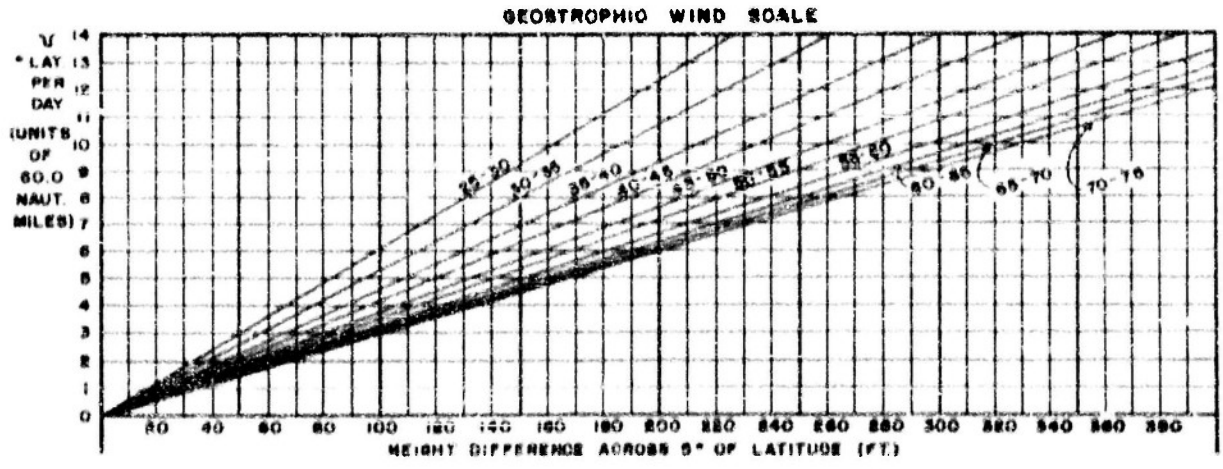

The geostrophic west-wind component *V*, given as a function of the height difference across five degrees of latitude for different latitude values (slanting lines).

Figure A2. Geostrophic wind-graph.

* These computations have been transmitted on a regular basis from the USAF Weather Central for several years.

respectively (northward decrease of heights giving positive values). This relation assumes that the meridional temperature gradient at 500 mb is the same as the meridional temperature gradient averaged between 500 mb and 900 mb, a good assumption.

A1.2. From the above equation and from the height and temperature averages at 5° latitude intervals at 500 mb, the height averages at 900 mb for 5° intervals are obtained. These values are entered into the geostrophic wind-graph (fig. A2) to give the average 900-mb geostrophic west-wind component at 5° latitude intervals. The west-wind component is given in units of latitude degrees per day (units of 90 nautical miles). The values of stationary wave length in longitude degrees can be obtained by entering the values of $\Delta\bar{h}_{900}$ into figure A3.

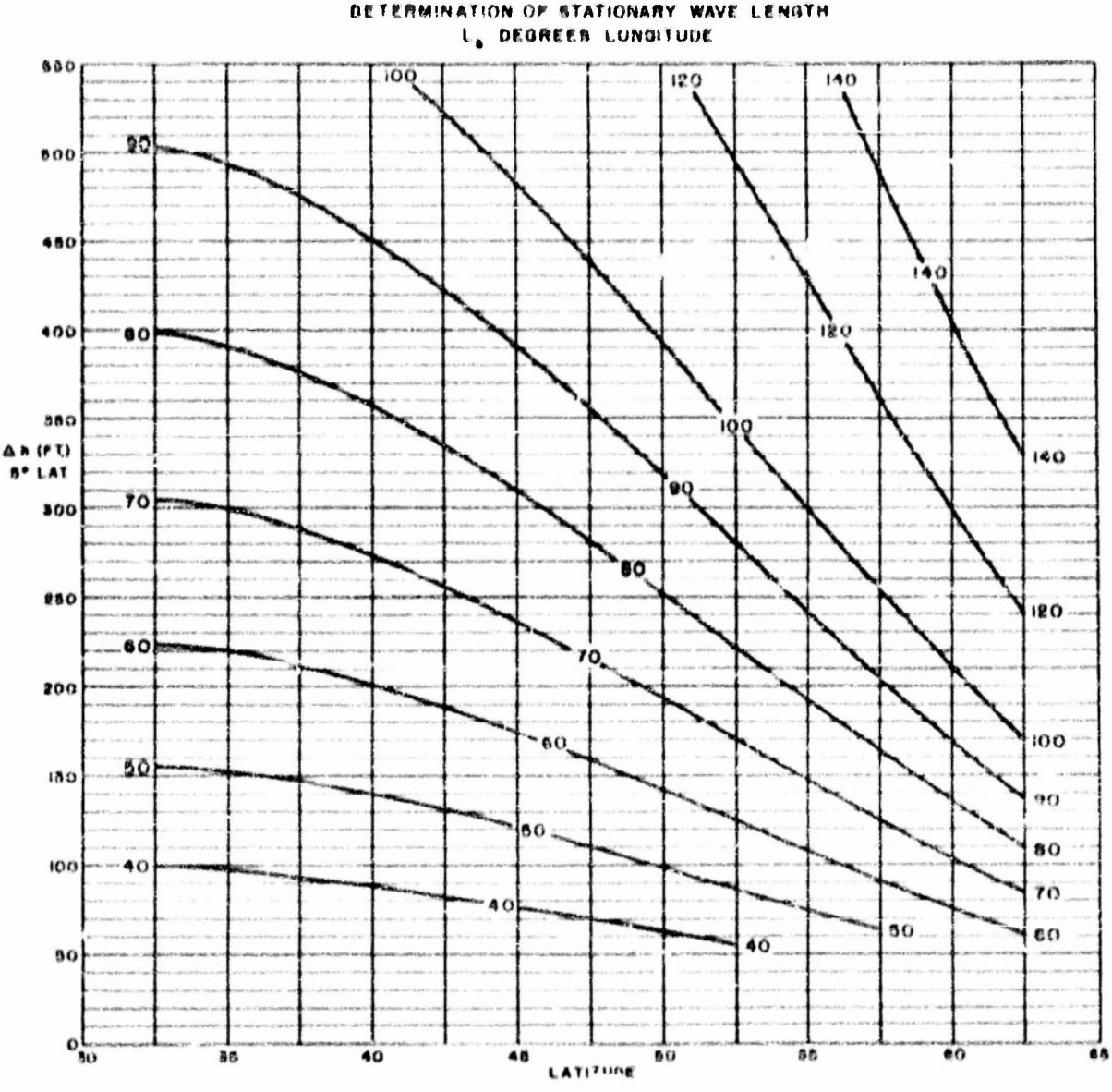

Figure A3. Stationary wave length (slanting lines) as a function of the average height difference across 5° of latitude ($\Delta\bar{h}$) and of the latitude.

A1.3. The following example is postulated to illustrate the various possibilities encountered in making these computations.

Latitude	λ_{max}	T_{max}
65	18102	−32.8
60	17923	−24.1
55	17885	−22.7
50	18165	−19.3
45	18527	−16.2

Latitude	$\Delta\lambda_{max}$	ΔT_{max}	$10\Delta T_{max}$	$\Delta\lambda_{min}$	V_{max}	L_s
60-65	179	1.3	23	147	4.7	
55-60	47	1.4	25	72	2.4	
50-55	280	3.3	59	221	8.0	70
45-50	362	3.2	58	304	11.8	83

A1.4. The computations should be made over a range of latitudes which includes the belt of westerlies. The values of L_s in these latitude bands can then be used for determination of the stationary wave length. The values of west-wind speed should be plotted in a suitable graph (see figure 4d), and connected by a smooth curve. The maximum value of stationary wave length will ordinarily be found at or just north of the same latitude as the maximum west-wind speed. This maximum value is then the representative stationary wave length for the west-wind current. On some occasions, a weak secondary current of westerlies to the north of the most prominent current will have the result of flattening the maximum on the west-wind profile. In such a situation the stationary wave length will increase northward, considerably north of the latitude of maximum westerlies. When this occurs, the representative value of L_s can be obtained from the h° zone corresponding to the maximum on the wind profile and to the center of the west-wind current on the maps.

A2.0. Computation of the Wave Speed. In the coordinate system of figure A4, the axes of which are the wave length and latitude, the curves of $\beta L^4/4\pi^2$ in units of longitude degrees per day have been entered. It is then evident from equation (3) that the speed c of a wave in longitude degrees per day can be obtained by subtraction of the value of $\beta L^4/4\pi^2$ from $\beta L_s^4/4\pi^2$, when L_s has been obtained as described previously, and L has been measured from the 500-mb chart at the latitude corresponding to the one at which L_s was selected. The wave speed then applies at the computation latitude.

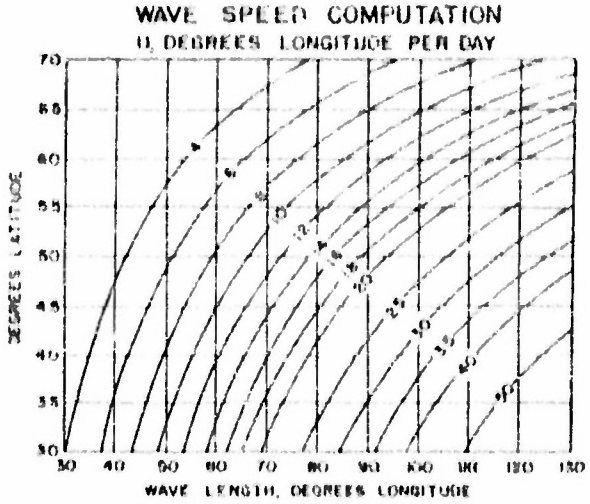

Figure A4. Diagram for determination of wave speed.

A2.1. When the motion of a major trough is desired, experience has shown that the use of the wave length to the next major trough upstream will give the best results.

A3.0. Construction of the Space-Mean and Vorticity Charts. With reference to figure 3 in the text, the procedure consists of first averaging the charts centered at A and C by adding graphically and dividing by two (see AWSM 105-50/2) to obtain a left-to-right (horizontal) average, and then averaging the charts centered at D and B for a vertical average (at right angles to the left-to-right average). The resulting horizontally and vertically averaged charts are then averaged to obtain the $\bar{Z}$ chart. The steps in detail follow:

a. Copy the 500-mb chart (referred to below as I), which has been carefully analyzed with contours at 200-ft intervals, on an acetate (II).

b. Over the 500-mb chart place the acetate copy displaced a distance of 720 nautical miles to the right. Place another acetate (III) over these, horizontally centered between them. On III draw contours at 200-ft intervals representing the average of I and II as displaced. Save Chart III, which represents the horizontal average.

c. Take Chart I again and place its copy, II, displaced this time a distance of 720 nautical miles at right angles to the displacement in step b. Place another acetate (IV) over these, centered between them. On IV draw contours at 200-ft intervals

representing the average of I and II as displaced. This represents the vertical average.

d. Center Chart IV on Chart III, with no displacement. Place a clean acetate (V) over these and draw contours at 200-ft. intervals representing the average of Charts III and IV. This is the desired space-mean chart.

e. The relative vorticity chart, $(\bar{Z} - Z)$ chart, is obtained by subtracting the starting 500-mb chart from the space-mean chart. It is helpful to put arrows on the $(\bar{Z} - Z)$ lines directed so that higher values lie to the left, indicating the sense of the flow.

A4.0. Solution of Pettersen's Wave-Speed Equation. A nomographic solution of Pettersen's wave-speed formula [23] has been prepared by Dr. R. D. Fletcher to obviate lengthy computations. This graph, figure A5, contains all solutions of the equation within what is considered a range of meteorological variables sufficiently wide for normal prognosis. Wave lengths up to 5000 nautical miles are considered, as are values of ϕ (angle of inclination of a wave axis from a meridian) up to 40°. Since the wind-speed range covers speeds between 80 knots from the east and more than 200 knots from the west, it is evident that solutions can be obtained for most current-case situations.

A4.1. When overlaid with an acetate, the nomograph for wave-speed calculation may be used as follows:

a. The wave length, L, measured in terms of either nautical miles or latitude degrees, is located on the top scale.

b. A wax-pencil line is drawn downward to the slanting line labelled 0°. If the wave axis tilts appreciably from the meridians, the wax-pencil line is continued downward a bit until it reaches the γ line corresponding to the tilt. It can be seen that the effects of tilt are relatively small. For most purposes acceptable accuracy is obtained by assuming zero tilt. This was done in the text (Section IIIB), where the tilt parameter was not discussed.

c. The wax-pencil line is then continued leftward to the appropriate ϕ line of latitude.

d. The wax-pencil line then is drawn downward until it reaches the proper wind speed, which is expressed in knots on this diagram.

e. The line again is extended to the left to the appropriate value of L/B. The L/B parameter is dimensionless, whence it must be remembered that B must be expressed in the same length units as L. (It should be noted that the wave speed is sensitive to the value of L/B. Also when B is infinite, the Pettersen equation reduces to the Rossby equation (1).)

f. To obtain the wave-speed, in units of either knots or latitude degrees per day:

(1) If the wax-pencil line lies *below* the axis labelled "Stationary Wave," it is extended upward to the wind-speed scale, on which the speed is expressed in either knots or latitude degrees per day. In this case the computed direction of wave movement is *eastward*.

(2) If the wax-pencil line lies *above* the stationary wave axis, it is extended downward to the wind-speed scale. Here, the computed direction of wave movement is *westward*.

A4.2. If map distances are measured in units of longitude degrees, slide-rule or tabular computations can be employed for conversion to units of latitude degrees. However, the upper portion of the nomograph can also be used, since the distance of one longitude degree equals the distance of one latitude degree multiplied by the cosine of the latitude (the top part of the nomograph is simply a graphical multiplication of distances by $\cos \phi$). The graphical procedure is as follows:

a. On the top "Latitude Degrees" scale locate the number of longitude degrees and extend a wax-pencil line down to the 0°-line.

b. Draw the line leftward to the appropriate latitude line, then carry it downward again to the 0°-line.

c. Extend the wax-pencil line again to the appropriate latitude line, then carry it upward to the top scale, which now will give the number of latitude degrees (at the pertinent latitude) equal in length to the number of longitude degrees measured on the map.

A4.3. Additional length and speed conversion factors are as follows:

Length		Speed	
1 statute mile	= 0.87 nautical miles	1 statute MPH	= 0.87 knots
1 kilometer	= 0.54 nautical miles	1 km per hr	= 0.54 "
1 lat. deg.	= 60 nautical miles	1 m per sec	= 1.94 "
		1 ft per sec	= 0.59 "
		1 lat. deg. per day	= 2.5 "

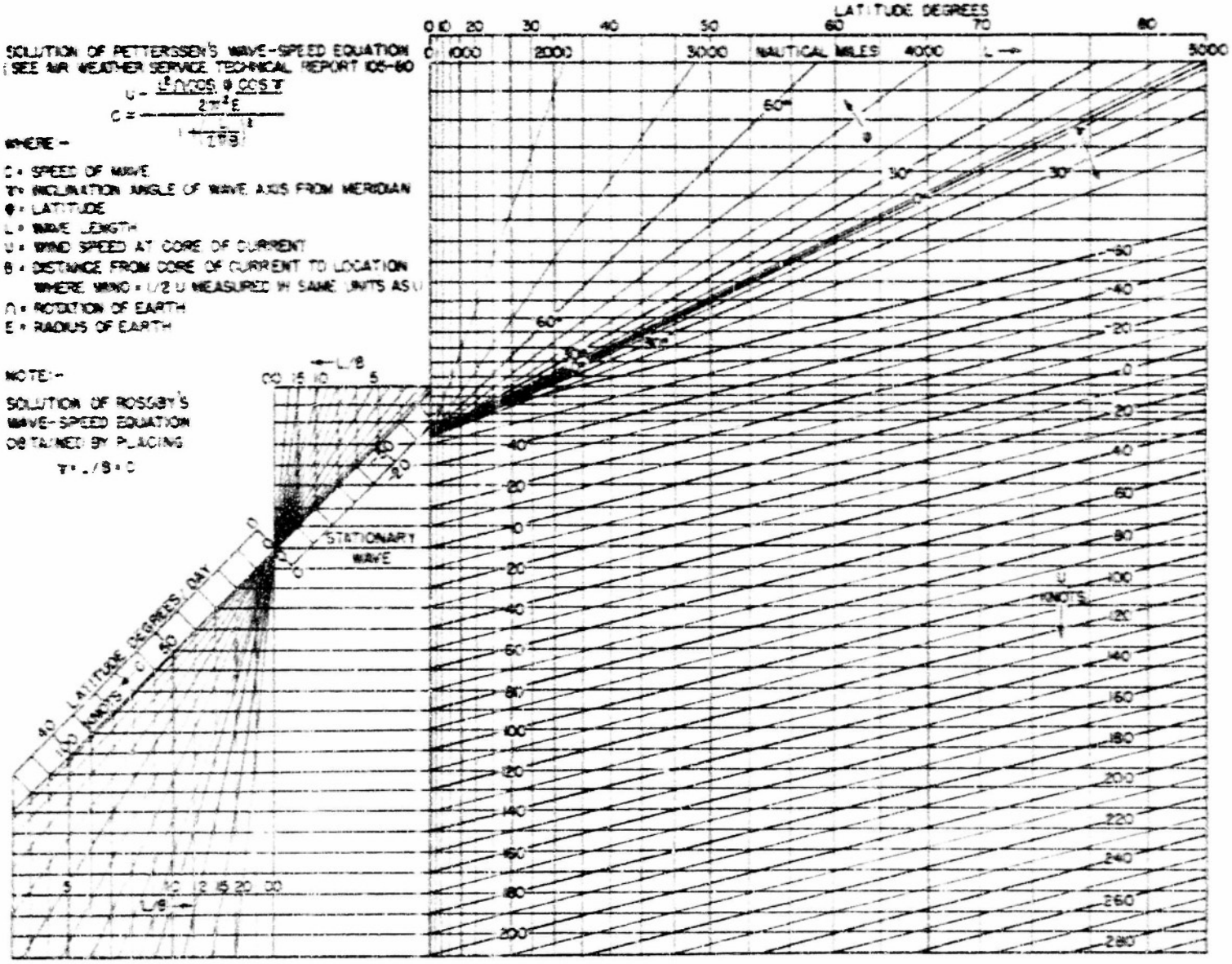

Figure A5. Nomogram for solution of Pettersseen's wave-speed equation.

(48 BLANK)

References

[1] Doffl, J. A., "Effect of the Andes Mountains on the General Circulation over the Southern Part of South America." *Bull. Amer. Meteor. Soc.*, Vol. 30, No. 7, pp. 242–247 (1949).

[2] Bolin, B., "On the Influence of the Earth's Orography on the General Character of the Westerlies." *Tellus*, Vol. 2, No. 3, pp. 184–195 (1950).

[3] Charney, J. G., "The Dynamics of Long Waves in a Baroclinic Westerly Current." *J. Meteor.*, Vol. 4, No. 5, pp. 135–162 (1947).

[4] Charney, J. G., "On a Physical Basis for Numerical Prediction of Large-Scale Motions in the Atmosphere." *J. Meteor.*, Vol. 6, No. 6, pp. 371–385 (1949).

[5] Charney, J. G., and A. Eliassen, "A Numerical Method for Predicting the Perturbations of the Middle Latitude Westerlies." *Tellus*, Vol. 1, No. 2, pp. 38–54 (1949).

[6] Charney, J. G., R. Fjörtoft and J. von Neumann, "Numerical Integration of the Barotropic Vorticity Equation." *Tellus*, Vol. 2, No. 4, pp. 237–254 (1950).

[7] Cressman, G. P., "On the Forecasting of Long Waves in the Upper Westerlies." *J. Meteor.*, Vol. 5, No. 2, pp. 44–57 (1948).

[8] Cressman, G. P., "Some Effects of Wave-Length Variations of the Long Waves in the Upper Westerlies." *J. Meteor.*, Vol. 6, No. 1, pp. 56–60 (1949).

[9] Cressman, G. P., "Variations in the Structure of the Upper Westerlies." *J. Meteor.*, Vol. 7, No. 1, pp. 39–47 (1950).

[10] Cressman, G. P., "An Application of Absolute-Vorticity Charts." *J. Meteor.*, Vol. 10, No. 1, pp. 17–24 (1953).

[11] Fjörtoft, R., "Numerical Method of Integrating the Barotropic Vorticity Equation." *Tellus*, Vol. 4, No. 3, pp. 179–194 (1952).

[12] Fultz, D., "Upper-Air Trajectories and Weather Forecasting." *Dept. Meteor., Univ. Chicago, Misc. Rept.*, No. 10, 121 pp. 1945.

[13] Hess, S. L., and S. M. Fonenko, "Constant Absolute Vorticity Trajectory Tables." *J. Meteor.*, Vol. 2, No. 4, pp. 238–245 (1945).

[14] Hovmöller, E., "The Trough-and-Ridge Diagram." *Tellus*, Vol. 1, No. 2, pp. 62–66 (1949).

[15] Haleh, Y., "An Investigation of a Selected Cold Vortex over North America." *J. Meteor.*, Vol. 6, No. 6, pp. 401–410 (1949).

[16] Johannessen, K. R. and Cressman, G. P., "Verification of an Equation for Trough and Ridge Motion." *Bull. Amer. Met. Soc.*, Vol. 33, No. 7, pp. 267–270 (1952).

[17] Carlin, A. V., "A Case Study of the Dispersion of Energy in Planetary Waves." *Bull. Amer. Met. Soc.*, Vol. 34, No. 7, pp. 311–318 (1953).

[18] Namias, J., *Methods of Extended Forecasting*. Washington, U. S. Department of Commerce, Weather Bureau, 64 pp. 1st ed., 1943; 2d ed., 1947.

[19] Namias, J., and P. F. Clapp, "Studies of Motion and Development of Long Waves in the Westerlies." *J. Meteor.*, Vol. 1, Nos. 3–4, pp. 55–77 (1944).

[20] Namias, J., and P. F. Clapp, "Normal Fields of Convergence and Divergence at the 10,000-foot Level." *J. Meteor.*, Vol. 3, No. 1, pp. 14–22 (1946).

[21] Palmén, E., "On the Origin and Structure of High Level Cyclones South of the Maximum Westerlies." *Tellus*, Vol. 1, No. 1, pp. 22–31 (1949).

[22] Palmén E., and C. W. Newton, "On the Three-Dimensional Motions in an Outbreak of Polar Air." *J. Meteor.*, Vol. 8, No. 1, pp. 25–39 (1951).

[23] Petterssen, S., "The Propagation and Growth of Jet Stream Waves." *Quart. Jour. Roy. Met. Soc.*, Vol. 78, July, 1952. Also see *AWS Tech. Report 105–80*, with Amendment No. 1, Nov. 1951.

[24] Platzman, G. W., "Some Remarks on the Measurement of Curvature and Vorticity." *J. Meteor.*, Vol. 4, No. 2, pp. 58–62 (1947).

[25] Rex, D. F., "Blocking Action in the Middle Troposphere and its Effect upon Regional Climate, I: An Aerological Study of Blocking Action." *Tellus*, Vol. 2, No. 3, pp. 196–211 (1950).

[26] Rossby, C.-G., "Relation between Variations in the Intensity of the Zonal Circulation of the Atmosphere and the Displacements of the Semi-Permanent Centers of Action." *J. Marine Res.*, Vol. 2, pp. 38–55 (1939).

[27] Rossby, C.-G., "Kinematic and Hydrostatic Properties of Certain Long Waves in the Westerlies." *Dept. Meteor., Univ. Chicago, Misc. Rept.*, No. 5, 37 pp., (1942).

[28] Rossby, C.-G., "Forecasting of Flow Patterns in the Free Atmosphere by a Trajectory Method," Appendix to: *Basic Principles of Weather Forecasting*, by V. P. Starr, New York, Harper & Brothers, pp. 268–284 (1942).

[29] Rossby, C.-G., "On the Propagation of Frequencies and Energy in Certain Types of Oceanic and Atmospheric Waves." *J. Meteor.*, Vol. 2, No. 4, pp. 187–203 (1945); "Dispersion of Planetary Waves in a Barotropic Atmosphere." *Tellus*, Vol. 1, No. 1, pp. 54–58 (1949).

[30] Rossby, C. G., "On the Dynamics of Certain Types of Blocking Waves." *J. Chinese Geophysical Soc.*, Vol. 2, No. 1, pp. 1–13 (1950).

[31] Starr, V. P.: "The Physical ... eral Circulation," in: *Cli... ...ology*, Amer. Met. Soc. ... 349.

[32] Stewart, H. J., "A Theory ... Obstacles on the Waves ... *J. Meteor.*, Vol. 8, No. 5, ...

[33] Staff Members, University ... ment of Meteorology. "... culation of the Atmosphe... tudes." *Bull. Amer. Me...* No. 8, pp. 285–279 (1947).

[34] Wilkins, E. M., "Relation ... Latitudinal Position of ... Westerlies and the Long... Ridges Aloft." *Univ... partment of Meteorology*, ... pp. (1949).

[35] Yeh, T., "On Energy ... sosphere." *J. Meteor.* ... 1–16 (1949).

[36] Sumner, E. J., "Cold Front ... Synoptic Study." *Met. ...* 82, pp. 201–301 (1953).

[37] Charney, J., and Phillips, ... Integration of the Quas... tions for Barotropic ... Flows." *J. Meteor.*, Vol. ... 90 (1953).

[38] Charney, J., "Numerical ... genesis." *Proc. Nat. ...* No. 2, pp. 89–110 (1954).

UNCLASSIFIED